Incipient vegetation recovery and its effect on braided channel morphology at Mount Pinatubo, Philippines

A THESIS
SUBMITTED TO THE FACULTY OF THE GRADUATE SCHOOL
OF THE UNIVERSITY OF MINNESOTA
BY

Emily O'Donnell Dunn

IN PARTIAL FULFILLMENT OF THE REQUIREMENTS
FOR THE DEGREE OF
MASTER OF SCIENCE

Dr. Karen Gran

June 2011

Acknowledgements

I would like to thank the numerous people who contributed or supported me in achieving this accomplishment. First and foremost, I would like to thank Dr. Karen Gran for her incredible guidance and support, as a mentor and a friend, during my time at UMD. I would also like to thank her for the amazing opportunity to travel to the Philippines.

A special thank you to my fiancée, Jakob, who is always relentless in his encouragement and support in everything I do.

I would also like to thank my committee, Dr. John Swenson and Dr. Pat Farrell for their attention and guidance. I would especially like to thank Dr. John Swenson for his leadership in numerical modeling.

I would like to thank Dr. Michal Tal for her guidance in my thesis work, her time she contributed in the field, and the opportunity to learn from her.

I would like to extend a special thank you to Josh Allen for his unbelievable help with my model and his patience through the whole ordeal.

I am grateful for the numerous people who helped conduct field work, especially Roy Tanglao and Edwin Manalang. I am incredibly appreciative of the all the support given to us by everyone at the Pinatubo Volcano Observatory.

Thank you to the USDA Agricultural Research Lab, most notably Natasha Pollen-Bankhead for her time and expertise.

I would like to thank my family (Mom, Dad, and Logan) for their love and support. Thank you to the Wartmans (Gretchen, John, and Sarah) for being my second family.

Lastly, I am grateful for the funding to complete this endeavor provided by the U.S. National Science Foundation grant EAR-0844241, the grant-in-aid from the Office of the Dean of the Graduate School of the University of Minnesota, and the UMD Department of Geological Sciences.

Abstract

Braided channels are characterized as being dynamic geomorphic agents whose behavior is somewhat unstable and unpredictable. Vegetation can provide stability to this unstable behavior, constraining lateral migration rates and providing resistance to flow. In this thesis I investigate the relationship between vegetation and braided channels to better understand what controls braided versus meandering channel morphology. More specifically, I am interested in the effects of vegetation including roughness and cohesion, how much vegetation is required to have an influence, and the effect of aggradation to predict the future of the braidplain on the Pasig-Potrero and Sacobia Rivers at Mount Pinatubo, Philippines.

The eruption of Mount Pinatubo in 1991 deposited 5-6 cubic kilometers of pyroclastic flow deposits onto the flanks of the volcano. I am studying the Pasig-Potrero and Sacobia Rivers on the east flank of Mount Pinatubo as vegetation becomes re-established in the braidplain. Vegetation was absent in the valley bottom for the first decade following the eruption due to extremely high sediment transport rates and rapid reworking of the braidplain. In the last three years vegetation has begun to persist in the braidplain through the rainy season.

Research procedures included a combination of field work and cellular numerical modeling. Field work was comprised of 76 1x1 meter plots to characterize vegetation growth, 181 root strength measurements, 15 root density samples, 52 Wolman pebble counts, and surface sediment samples for grain size analysis. A fiber bundle model, RipRoot, devised by Pollen and Simon (2005) was utilized to obtain values for added cohesion due to roots present on streambanks. Roughness was quantified for different vegetation growth scenarios. A cellular numerical model was devised, based on Murray and Paola (2003), to test field data and gain more understanding of the relationship between vegetation and channel dynamics. Water and sediment were routed through a 200x42 cellular matrix based on slope and stream power, respectively. Vegetation

was added as an impedance to sediment transport, which can also be thought of as an increase in bank strength.

Both braidplains range in with from 300-500 meters, with an average of 10-50 braids, 0.1-20.0 meters wide, in cross-section. Vegetation growth occurs in patterns categorized as sparse, dense and clumpy comprised of a mix of grasses, vines, forbs and woody trees. Both stem diameter and height increased from sparse to clumpy to dense vegetation, with an average diameters of 5.25 mm in sparse to 9.92 mm in dense plots and average stem heights from 0.72 m in sparse to 2.44 m in dense plots. Roughness calculations show that vegetation decreases flow velocities by an estimated 3-12%. Values obtained from RipRoot show that dense vegetation adds 8.21-12.31 kPa of cohesion to streambanks while sparse vegetation adds 0.13-0.29 kPa. This added cohesion creates stable streambanks, which otherwise are considered unstable. Cellular model results run with the effect of vegetation show more organization of flow, seen as a decrease in total channel width and an increase in channel depth. Channel width decreases with increasing vegetation density. Channel width increases with increasing sediment transport rates, lending the idea of a sediment transport threshold that must be overcome for vegetation growth to occur on the braidplain. This observation is compatible with field observations showing a lack of vegetation growth in the braidplain while fluvial aggradation rates were high. In all, field data and observations, coupled with model results show that vegetation increases bed roughness and increases bank strength, effects that are consistent with evolution to a single-thread channel pattern.

Table of Contents

List of Tables

List of Figures

1.0 INTRODUCTION

Braiding is the main mode of instability for unconstrained flow over non-cohesive sediment (Schumm et al., 1987; Thorne, 1990; Murray and Paola, 1994; Gran and Paola, 2001; Murray and Paola, 2003; Tal et al., 2004). Braided rivers act as dynamic geomorphic agents, characterized as having somewhat unpredictable behavior as their braids split and rejoin while actively migrating across their braidplain. It has been shown that vegetation can act as a means of stability to this unstable behavior, providing a mechanism for braided rivers to evolve into single-thread channels (Schumm et al., 1987; Thorne, 1990; Murray and Paola, 1994; Gran and Paola, 2001; Tal et al., 2004). Thus, better quantifying the relationship between channel dynamics and vegetation is fundamental to understanding what controls braided versus meandering channel morphology.

Vegetation affects lateral braidplain migration by strengthening banks and slowing flows, directly opposing the tendency of braided rivers to migrate freely across their braidplain. Banks are strengthened through root binding and the deposition of fine-grained cohesive sediment (Wu et al., 1979; Greenway, 1987; Thorne, 1990; Gran and Paola, 2001; Micheli and Kirchner, 2002; Murray and Paola, 2003; Tal and Paola, 2007; Pollen-Bankhead and Simon, 2009). This increases the threshold shear strength required to initiate sediment transport (Wu et al., 1979; Gran and Paola, 2001; Wynn et al., 2003; Tal et al., 2004; Tal and Paola, 2007; Baets et al., 2008). Vegetation increases flow resistance by increasing drag and reducing the local velocity, thus decreasing the fluid stress available for erosion and transport (Thorne, 1990). Vegetation adds roughness to a fluvial system as individual stems and clumps are able to choke off weaker channels and corral the flow into fewer, stronger channels with more uniform higher velocities (Tal et al., 2004). In an aggrading system, there is an additional barrier to vegetation growth, and thus braiding may be encouraged due to high

sedimentation rates. This study explores the role of vegetation in an active aggrading braidplain as vegetation and channel dynamics co-evolve.

Mount Pinatubo in the Philippines is an ideal location to better understand the coupling between vegetation and braided channel dynamics in active aggradational systems (Figure 1-1). The eruption of Mount Pinatubo in June of 1991 deposited 5-6 cubic kilometers of pyroclastic flow deposits onto the flanks of the volcano (Scott et al., 1996). Due to extremely high sediment transport rates and rapid reworking of the braidplain, many streams have persisted as braided channels across large floodplains, un-vegetated and choked with sediment. The two watersheds I will be focusing on, the Pasig-Potrero and Sacobia Rivers, experienced 1.1 – 1.3 km^3 of sediment deposition, primarily from pyroclastic flow deposits (Major et al., 1996; Scott et al., 1996; Daag, 1994). The deposited sediment, containing 70-85% sand, covered approximately 30% of each basin, directly influencing their recovery rate. Aggradation rates in the Pasig-Potrero have decreased from 5 meters/year in 1997 to 0.7 meters/year in 2002-2009 (Gran et al., 2011). In the past few years, vegetation is finally beginning to return to the braidplain and sustain through the rainy season, constraining not only the location of the flow but also the amount of sediment moving downstream. Vegetation currently consists primarily of sparse grasses with distinct patches of older, dense mixes of grasses, vines, trees and forbs.

By quantifying the effects of vegetation locally, prediction as to the trajectory of channel migration and evolution is hypothesized for different growth scenarios in braided systems. This was accomplished by experimenting with a 2-D cellular model. By varying channel dynamics as well as vegetation growth rate and patterns, we are able to understand how the co-evolution of the two may shape the future of the Pasig-Potrero and Sacobia braidplains as aggradation rates decline.

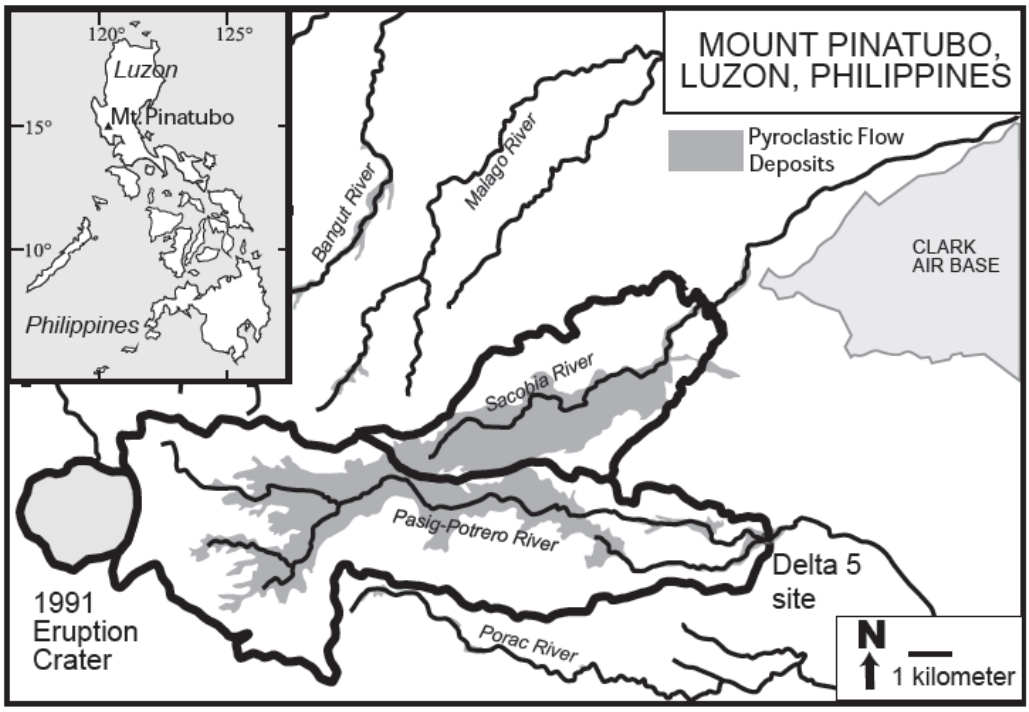

Figure 1-1. This thesis research area is located on the east flank of Mount Pinatubo on the island of Luzon, in the Philippines. Vegetation recovery is being studied in two rivers, the Pasig-Potrero and the Sacobia.

2.0 BACKGROUND

2.1. BRAIDED RIVER DYNAMICS AND VEGETATION

Braiding is the main mode of instability for unconstrained flow over non-cohesive sediment; it acts as a "default" mode for fluvial systems (Tal et al., 2004). Braided channels are complex geomorphic agents that migrate laterally, split, rejoin, and develop bars, continuously shifting and varying flow (Murray and Paola, 1994). In such dynamic systems it has been found that meandering rivers can result from partial suppression of braiding instability through the introduction of vegetation (Murray and Paola, 1994; Tal and Paola, 2007). Vegetation decreases lateral mobility and migration rates, making channels more stable. It also decreases braiding intensity and total wetted width, thus decreasing the number of active channels and making existing channels narrower and deeper (Gran and Paola, 2001; Tal et al., 2004). Braiding intensity is a method to describe how intensely braided a channel is, categorized either as the mean number of active channels across a channel belt or the ratio of the sum of channel lengths in a reach to reach length (Knighton, 1998). As vegetation begins to colonize areas of low discharge it seems to have a ratchet effect, meaning that once vegetation has taken hold, its effects are not easily reversed, even if the discharge of the channel returns to its previous level. Vegetation decreases the variability of stream discharge in individual braids as smaller, weaker, channels are choked off and more consistent channels with higher discharge form (Gran and Paola, 2001; Tal et al., 2004; Tal and Paola, 2007).

Vegetation constrains traditional braided river behavior through three main processes: 1) it acts as the primary source of cohesion as roots strengthen banks; 2) vegetation induces trapping of fine-grained silts and clays, also increasing cohesion; 3) stems increase bed roughness, decreasing the shear stress (τ) available to transport sediment (Figure 2-1). Numerous field studies have looked at individual components of these effects such as bank and root strength;

Figure 2-1. Vegetation has two main effects on the braidplain: (A) vegetation increases roughness, providing resistance to flow; and (B) cohesion is added by root networks and the increased deposition of fine-grained, cohesive sediment. Increased cohesion increases bank strength.

(Abernathy and Rutherford, 1998; Abernathy and Rutherford; 2000; Abernathy and Rutherford, 2001; Easson and Yarbrough, 2002; Simon and Collison, 2002; Pollen and Simon, 2005; Pollen, 2007; De Baets et al., 2008; Simon et al., 2008; Pollen-Bankhead, 2009) and the effects of roughness (Stone and Tao Shen, 2002; Thompson et al., 2004; Huthoff et al., 2007; James et al., 2008). In addition, flume and modeling experiments have been utilized to better define the integrated effects of vegetation and channel morphology (Gran and Paola, 2001; Micheli and Kirchner, 2002; Murray and Paola, 2003; Tal et. al., 2004; Wynn et al., 2004; Coulthard et al., 2006; Wynn and Said, 2006; Tal and Paola, 2007; Van De Wiel and Darby, 2007; McBride et al., 2008; Braudrick et al., 2009).

Using flume experiments and alternating discharge with plant seeding and growth researchers have been able to evolve braided river systems into self-maintained single-thread channels with well-defined banks and floodplain (Gran and Paola, 2001; Tal et al., 2004; Tal and Paola, 2007). A key to this success has been varying stream and sediment discharge, giving plants a chance to colonize freshly deposited sediment (Tal and Paola, 2007). This observation, of an increase in vegetation density often coinciding with lesser stream discharge rates, has also been documented in natural rivers (Eschner et al., 1983; Tal et al., 2004).While these results are valuable, researchers have also documented variations in results occurring due to natural variations in fluvial systems. For example, Pollen (2007) found that soil and root moisture can affect the ability of roots to add cohesion and increase bank strength. Other studies have found that bank height plays an important role in root reinforcement; most reinforcement occurs in the upper meter of soil (De Baets et al., 2008; Abernathy and Rutherford, 2000; Pollen, 2007), and 75% of all roots are concentrated in the upper 30 cm of the stream bank (Wynn et al., 2004).

2.2.1. ROUGHNESS

Vegetation increases roughness of the channel, interacting directly with the flow. Vegetation enhances bed roughness by increasing flow resistance, and therefore reducing velocity and increasing flow depth (Liu et al., 2008). The influence of vegetation on flow is a function of vegetation height, size, flexibility, and density as well as flow depth and velocity (Ghisalberti, 2002). If plants are emergent and plant height exceeds flow depth, the stems exert a drag force on the fluid. This is a function of the flow velocity, a drag coefficient, and the vegetation density. As a result, due to the increased drag, the velocities of flow decrease (Wilson et al., 2003; Stoesser et al., 2009; Liu et al., 2010). If the vegetation is spaced far enough apart that the wakes formed downstream from each stem does not interact with each other, the coefficient of the drag is similar to that of an individual cylinder set in the flow (James et al., 2008). If stems are placed close together, their individual wakes can interact, lowering the bulk drag coefficient. Therefore, the bulk drag coefficient is higher in sparse vegetation and then slowly decreases as vegetation density increases (Stoesser et al., 2009; Liu et al., 2010).

As flow velocity increases stems have the tendency to bend, eventually becoming submerged, and the effect they have on flow characteristics changes (Huthoff, et al., 2007). Submerged stems exert less drag than emergent stems. The amount of flow resistance in submerged vegetation is dependent on plant height. Therefore, as flow velocity increases, the amount of bending increases, affecting the flow resistance and velocity (Stone and Tao Shen, 2002; Thompson et al., 2004).

In this study, for the purposes of tall, emergent, sparse vegetation, stems are treated as individual cylindrical rods imparting a drag force on the flow (Stone and Tao Shen, 2002) (Figure 2-2). First, consider an open channel with emergent vegetation in the form of cylindrical stems of equal length distributed evenly over the bed. The total shear stress in the system can be expressed as:

$$\tau_w = \tau_v \tau_b \quad (1)$$

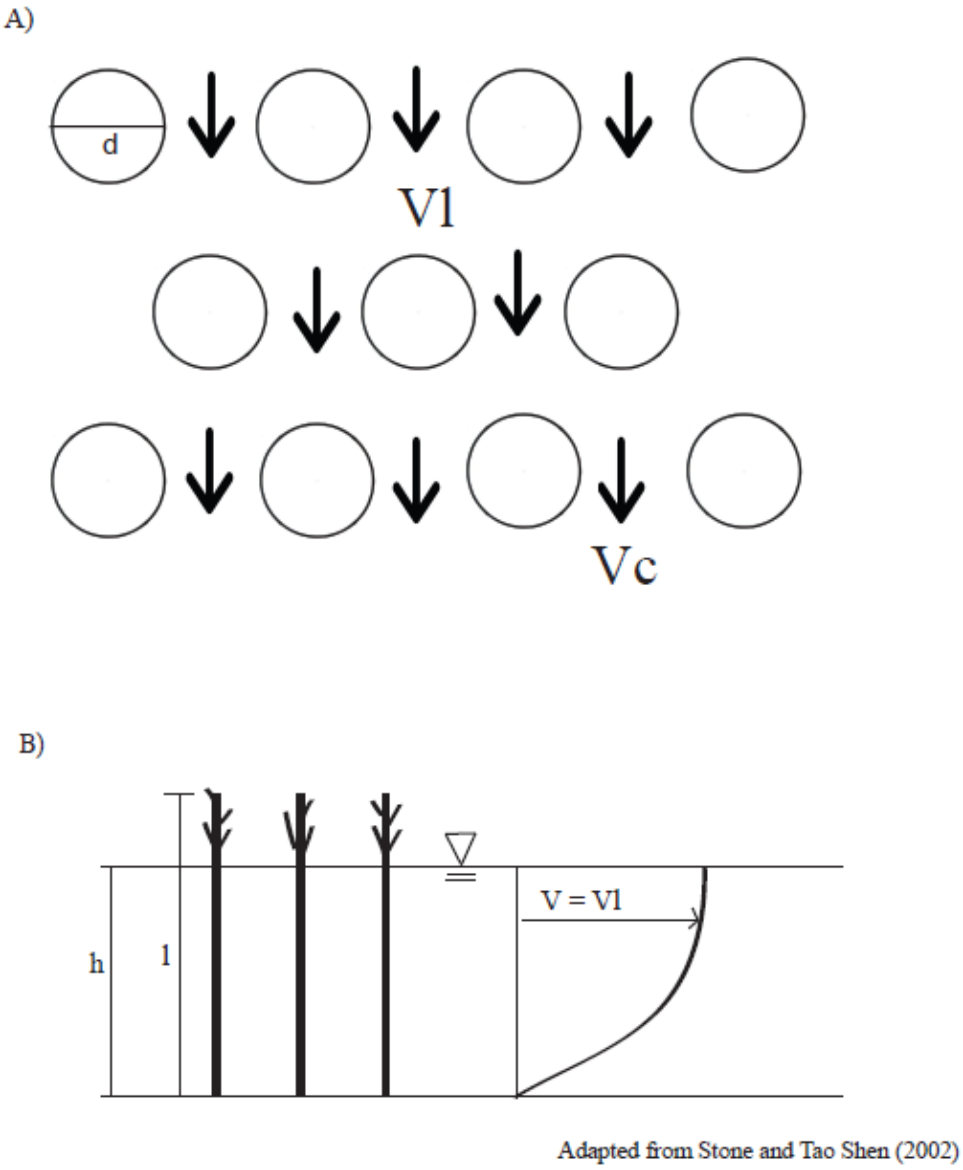

Figure 2-2. (A) Definitions of V_c and V_l in the vegetation layer as defined by the cellular model. (B) Definition sketch for open channel flow with emergent cylindrical vegetation.

where τ_w is the streamwise component of shear stress, a function of τ_v (the resistance due to the drag around the cylinders within the stem layer) and τ_b (shear stress taken up by the bed). In many vegetated cases τ_b is insignificant, and can thus be ignored, compared to the resistance due to vegetation (Stone and Tao Shen, 2002). The reach-average shear stress term can also be expressed as the more familiar depth-slope product:

$$\tau_w = \rho g S h (1 - \gamma l^*) \tag{2}$$

where ρ is the density of water, g is the acceleration due to gravity, S is the channel slope; h is the flow depth; γ is the area concentration of stems; and l^* is the wetted stem length/flow depth ratio, which is equal to one in emergent cases. The fraction of the bed that is occupied by vegetation is: $\gamma = N\pi d^2/4$, where N is the number of stems per unit bed area and d is the stem diameter.

The stem drag force per unit bed area is expressed as:

$$\tau_v = \frac{1}{2}\rho C_D N d l V_c^2 \tag{3}$$

where C_D is the drag coefficient for a single cylinder, having the value of 1.05 for grass-like cylindrical vegetation (Stone and Tao Shen, 2002; Thompson et al., 2004; Huthoff et al., 2007 James et al., 2008), l is the wetted stem length, and V_c is the average velocity in the stem layer at the constricted section (Figure 2-2).

Equation (3) shows the drag force as a function of V_c. However, Stone and Tao Shen (2002) explain that the term V_l, apparent vegetation velocity, is more useful because it quantifies the average velocity everywhere in the presence of vegetation. The relationship between V_c and V_l can be obtained from the continuity of flow in the stem layer, $V_l B = V_c B_c$, where B is the channel width and B_c is the minimum channel flow width in the stem layer. Therefore:

$$V_l = V_c(1 - d\sqrt{N}) = V_c\left(1 - \sqrt{\frac{4\gamma}{\pi}}\right) \quad (4)$$

By combining equations (1) – (3), V_l can also be written as:

$$V_l = \left(1 - \sqrt{\frac{4\gamma}{\pi}}\right)\sqrt{\frac{g(1-\gamma l^*)d\pi}{2\gamma l^* C_D}}\,\sqrt{S} \quad (5)$$

Equation (5) can be rewritten in terms of V_c by using equation (4):

$$V_c = \sqrt{\frac{(1-\gamma l^*)}{\frac{1}{2}C_D l^*}\frac{g}{Ndh}}\,\sqrt{hS} \quad (6)$$

To relate V_c (the average velocity in the stem layer at the constricted section), to V_l the apparent channel velocity) equation (6) can be rewritten by introducing equation (4) so that:

$$V_c = \frac{V_l F_v}{(1-dl^*\sqrt{N})} \quad (7)$$

where F_v is 1.0 (Stone and Tao Shen, 2002). Therefore, by combining equation (6) and (7) an equation for the apparent channel velocity can be obtained, in the form of:

$$V_l = \frac{(1-dl^*\sqrt{N})}{F_v\sqrt{l^*}}\sqrt{\frac{(1-\gamma l^*)}{\frac{1}{2}C_D}\frac{g}{Ndh}}\,\sqrt{hS} \quad (8)$$

Equation (8) can be used to obtain a value for the apparent channel velocity with vegetation (Stone and Tao Shen, 2002). Symbols used are defined in Appendix A.

2.2.2. COHESION

Vegetation increases cohesion which enhances bank strength. Bank strength is increased by roots and the deposition of fine-grained silts and clays. Soil without roots has high compressional strength but little tensile strength. When roots are added to the soil they add tensile strength. Roots also add elasticity which helps to distribute stresses throughout the soil; this increases the bulk shear stress of the soil. Thus soil is allowed to behave as a cohesive body (Thorne, 1990). Increased bank strength increases the critical shear stress (τ_c) required to begin eroding the bank. An increase in τ_c on the bank can lead to an increase in bank angle, allowing for a deeper and narrower channel to develop (Abernathy and Rutherford, 2001; Wilson et al., 2003; De Baets et. al., 2008; Stoesser et al., 2009; Liu et al., 2010).

The effect of roots has been undertaken by several research groups (Abernathy and Rutherford, 2001; Simon and Collison, 2002; Pollen and Simon, 2005; Pollen, 2007; De Baets et al., 2008; Simon et al., 2008). The tensile strength of roots as well as forces necessary to pullout and break roots has been tested. Root tensile strength has been found to decrease with increasing root diameter following a power law (Pollen, 2007; De Baets et al., 2008). With smaller root diameters, breaking forces exceed pullout forces and vice versa for large root diameters. In addition, a threshold diameter exists between root pullout force and root breaking force that varies with soil shear strength (Pollen, 2007). Root tensile strength values have been found to vary from 25-300 MPa depending on species (De Baets et al., 2008).

Several methods have been used to quantify the amount of cohesion roots add to a soil matrix. The first attempt was made by Wu et al., (1979) who utilized a perpendicular model to quantify the added cohesion. In such a model:

$$\Delta S = T_r \left(\frac{A_R}{A}\right) * 1.2 \quad (9)$$

where ΔS is the increased shear strength due to roots, and T_r is the average tensile strength of roots per unit area of soil. $\frac{A_R}{A}$ is the root area ratio, where A_R is the area of soil occupied by roots, and A is the total soil area. In this model, the magnitude of root reinforcement depends on the amount of roots present in the soil. Several studies have shown that this simple perpendicular model overestimates root reinforcement because it assumes all of the roots break at the same time and that their full tensile strength is mobilized at the breaking point (Simon and Collison, 2002; Pollen and Simon, 2005; Pollen, 2007; De Baets et al., 2008; Simon et al., 2008). In addition these studies recognize that, while such measurements can be made in the field, several variables can heavily influence a data set, such as root and soil moisture (Pollen and Simon, 2005).

Pollen and Simon (2005) recognized the overestimation of this perpendicular model and thus attempted to correct its mains source of error. They derived a more complex relationship for root reinforcement utilizing a fiber bundle model approach, embodied in their RipRoot model (Pollen and Simon, 2005). RipRoot takes into account the fact that roots within a soil matrix have varying tensile strengths and therefore break at different times when a load is applied to the soil. In addition, the model evenly redistributes the load from the broken roots at each step to the remaining intact roots crossing the shear surface. While the model still makes assumptions, for example: 1) that the elastic properties of fibers are the same and that the fibers are all parallel to each other in the direction of loading, and 2) that the load is evenly distributed to remaining roots following breakage, it successfully reduces the overestimations from Wu et al., 1979 (Pollen and Simon, 2005).

Input values for the model are based on the root diameter and tensile strength relationship of a specific plant species, in the following form:

$$T_r = ad^{-b} \tag{10}$$

where root tensile strength, T_r is shown to decrease with increasing root diameter, d, (Mattia et al., 2005; Tosi, 2007; DeBaets et al., 2008). Values a and $-b$ are empirically-derived coefficients that describe the relationship between root diameter and tensile strength in the RipRoot model. The number and size of roots in 1 square meter of bank face is also input into the model.

2.2. NUMERICAL MODELING OF BRAIDED RIVERS

Modeling river morphology is useful to gaining more understanding of the interactions between discharge, sediment, vegetation and other variables governing channel dynamics. Murray and Paola (1994) were the first to utilize cellular modeling to explain braided channel morphology. Cellular-based models use simple rules to replicate dynamics of a system (Murray and Paola, 1994; Murray and Paola; 1997; Nicholas, 2005; Coulthard et al., 2006; Thomas et al., 2007). One advantage of cellular modeling stems from its flexibility; it takes a first principles approach, including only what is necessary to explain behavior of a natural system (Murray and Paola, 2003).

The cellular model of Murray and Paola (1994) is a simple deterministic numerical model of water flow over a noncohesive bed that captures the main spatial and temporal features of real braided rivers. It is a variation of the coupled map lattice model of dynamical systems research (Murray and Paola, 1997). The model suggests that the only factors essential for braiding are bedload sediment transport and laterally-unconstrained surface flow. From the model, patterns arose from local scour and deposition caused by a linear dependence of bedload sediment flux on water discharge (Murray and Paola, 1994).

The initial conditions of the model begin with uniform slope and white noise elevation perturbations with amplitude of the order of the average downhill elevation difference between adjacent rows of cells. The uphill and downhill ends of the lattice will remain fixed throughout the runs. Iteration of the model begins with water being introduced to the system carrying sediment. During the iteration

water is routed to 1-3 downstream neighbors, in order to simplify the algorithm. Water coming into one to three of the neighboring cells is governed by:

$$Q_w = \frac{Q_o \ S_i^n}{\sum S_i^n} \tag{11}$$

where S_i is the slope between cells, Q_w is the amount of water input into each cell, and Q_o is the amount of water already there. The summation normalizes the discharge so all water coming in at the beginning of an iteration leaves at the end (Murray and Paola, 2003).

Sediment is also routed in the model, using two different methods. First, through normal bedload transport, the amount of sediment routed to each cell, Q_s, is determined by the stream power index, using the equation:

$$Q_s = W[Q_w \ (S_i + \ C_s) - \ T_h \ ]^m \tag{12}$$

where the exponent m is based on empirical data relating sediment transport to steam power using reach-averaged slopes (Murray and Paola, 2003). C_s is a constant defined crudely as three times the average slope allowing sediment transport on locally flat or uphill areas. W is a constant, and T_h is a sediment-transport threshold (Murray and Paola, 1994). The value $T_h$can model cohesion as an increase in critical shear stress, making erosion processes more difficult.

Murray and Paola (2003) route sediment laterally based on a parameter developed by Parker (1984) but simplified it to ignore the dependence on shear stress. Instead, if the lateral neighbor cell has a higher elevation than the cell in question, an amount of sediment, Q_{sl}, is transported down the lateral slope by:

$$Q_{sl} = \partial S_i \, Q_s \tag{12}$$

where ∂ is a constant, adjusted so that Q_{sl} is a few percent of the sediment transport in the cell in question, Q_s, roughly consistent with the previous equation (Murray and Paola, 1997). Iteration ends when water reaches the downstream end of the lattice. The elevation of each cell is then adjusted according to the difference between the total sediment loads entering and leaving each cell (Murray and Paola, 1994).

Murray and Paola (2003) then modified this model to examine the effect of sediment stabilization by roots on the channel pattern of rivers. This was the first of its kind to incorporate the effects of vegetation in such a model, via simple rules for vegetation growth such as destruction, growth, and sediment stabilization. To introduce vegetation the model followed several simple steps. Plant growth was added in two ways: 1) an impedance of sediment transport (Q_s) as is caused by the development of protective surface vegetation; 2) the increase in bank strength from roots and thus the decrease in lateral sediment transport (Murray and Paola, 2003). In this way if plants are growing in a cell next to a channel, a steeper slope can develop and be maintained longer between the vegetated cells and the adjacent channel cell (Tal et al., 2004). Vegetation was destroyed following two conditions: 1) the rate of deposition of sediment rose above a certain value; 2) the erosion rate rose above a certain value (Murray and Paola, 2003). The model found that vegetation enhances bank resistance to erosion, causing development of single-thread channels (Murray and Paola, 2003).

Application of additional cellular models in a range of fluvial environments has also been experimented with (Brookes et al., 2000; Murray and Paola, 2003; Thomas et al., 2004; Tal et al., 2004; Nicholas, 2005; Coulthard et al., 2006). For example, Thomas et al., (2004) found that increased sediment supply leads to aggradation, an increase in braid intensity and, to a lesser extent, an increase in channel width. In addition, Nicolas (2005) and Thomas et al., (2004) found that using cellular modeling helped to bring out complexities of the

relationship between surface age distributions and the time period since of the occurrence of substantial morphological change in braided rivers.

3.0 FIELD SITE

The study area, comprised of the Pasig-Potrero and Sacobia Rivers, drains the east flank of Mount Pinatubo, on the island of Luzon in the Philippines (Figure 1-1). The June 1991 eruption left these river valleys partially buried with as much as 200 m of loose pyroclastic debris (Major et al., 1996; Scott et al., 1996) (Figure 3-1). The climate in the area is tropical and monsoonal, with distinct rainy and dry seasons. Nearby Clark Air Base on the lower east flank of the volcano receives an average yearly rainfall of 1,950 mm, 60% of which falls July-September (Scott et al., 1996). Frequent heavy rainfall coupled with fine-grained loose sediment from the eruption has triggered many large lahars since 1991 (Major et al., 1996; Scott et al., 1996; Tuñgol, 2002).

These events have left these rivers with several unique features which are changing somewhat rapidly as the braidplains evolve through time. The average slope at the alluvial fan head is 2%. Sediment deposition on the Pasig-Potrero and Sacobia fans peaked in 1991 at >3.1 x 10^6 $m^3 / km^2 /year$ and has decreased over time. In 1997, when the last major lahar even occurred, sediment deposition was estimated at 0.45 x 10^6 $m^3 / km^2 / year$ (Tuñgol, 2002). Median surface grain size (D_{50}) has increased over time as the channel bed coarsens and the system flushes itself of fine-grained sediment. On the Sacobia the D_{50} value at the mouth of the braidplain has changed from -2.3ϕ (5 mm) in 1997-8 to -4.6ϕ (24 mm) in 2000-02. At the mouth of the braidplain on the Pasig-Potrero it has evolved from -2.8ϕ (7 mm) in 1997-98 to -5.2 ϕ (37 mm) in 2000-02 (Gran and Montgomery, 2005).

Field observations from the 2009 rainy season show that the Sacobia and Pasig-Potrero braidplains are comprised of shallow braids ranging from a few

Figure 3-1. The eruption of Mount Pinatubo in 1991 deposited 5-6 cubic kilometers of pyroclastic flow deposits onto the flanks of the volcano, leaving the river valleys partially covered with as much as 200 meters of loose pyroclastic debris (Scott et al., 1996).

centimeters to a few meters in width, continuously moving across the braidplain and transporting sediment. Occasional higher flow allows the channels to rise high enough to either completely fill the valley bottom or develop roll waves. During low-flow rainy season conditions, the average water depths are usually <10cm yet the flow is able to transport clasts with diameters twice the flow depth as recorded in previous years by Montgomery et al. (1998) and Gran et al (2006). Previous rainy season conditions have wiped out vegetation growth on the braidplain (Gran and Montgomery, 2005); however, field observations from 2009 reveal that vegetation was able to persist through the rainy season.

During the 2010 dry season we observed similar characteristics on the Sacobia River. However, channel incision of 1-3 meters was observed on the Pasig-Potrero River in areas that, four months earlier, were braided. Suspended load and bedload transport also decreased significantly in the dry season. This area is unique in terms of its high precipitation coupled with sediment characteristics. It is ideal for such as study as the rivers are beginning to coarsen and vegetation is starting to persist in the channel through high flow events, having a direct effect on channel planform (Figure 3-2).

Vegetation growth on the Sacobia and Pasig-Potrero braidplains is relatively young, only occurring within the last three years (Figure 3-2). The dominant vegetation species identified include grasses (*Saccharum spontaneum, Miscanthus floridulus, Phragmites karka,* and *Melinis repens*), vines (*Centrosema molle* and *Calopogonium mucunoides*), forbs (*Chromolena ordata*), and woody trees (*Parasponia Rugosa*). The most dominant species, *Saccharum spontaneum*, is a reed-like grass related to sugar cane and composes approximately 85% of the vegetation present on the braidplain. Vegetation is composed mainly of colonized vegetated islands, occasionally located on banks 0.3-1.5 meters high.

Figure 3-2. (A) The Pasig-Portero braidplain in 2002, 11 years post-eruption. The eruption left, the once single-threaded channels, highly dynamic braided systems choked with sediment. The frequently reworked, dynamic floodplains are somewhat unpredictable. (B) The Pasig-Portero braidplain in August 2009, 18 years post-eruption. During the past three years vegetation has started to persist through the rainy season and constrain not only the location of flow but possibly the amount of sediment moving downstream.

4.0 METHODS

4.1. FIELD/DATA COLLECTION

Mount Pinatubo in the Philippines provides an ideal field site for examining the interaction between vegetation and braided rivers; especially the Pasig-Potrero and Sacobia Rivers, as they received some of the largest volumes of sediment deposition after the eruption. These braidplains readily illustrate the dynamic nature of braided rivers through seasonal changes in vegetation growth and channel patterns. Two field excursions occurred to collect data and observations concerning the interaction of vegetation and braided rivers, one in August 2009 (the rainy season) and the second in January 2010 (the dry season). Data collected fall into two categories: 1) quantifying the vegetation and; 2) describing the channel dynamics. Together these data help to characterize the system and quantify the processes occurring in the braidplain to inform the use of these variables in the cellular model.

The first group of data was collected to quantify the vegetation. Vegetation patterns were classified as dense, clumpy and sparse (Figure 4-1). This classification scheme arose from aerial photographs taken during the summer of 2009 and ground field observations. Within each vegetation pattern, data were collected in a series of 76 ground-referenced 1 m^2 plots. Plot data were collected by setting up a ruler to define 1 m^2 to define a plot. In each plot the substrate type, location and bank height (if relevant) were recorded. Each species present in the plot was identified and the following information recorded: stem count, stem diameter, stem height, and percent cover (0-25%, 25-50%, 50-75%, and 75-100%). These data were combined and used to define the basic characteristics of each vegetation class.

Root tensile strength and stress displacements were measured using a device called a Root-Puller. This device was constructed by the Agricultural Research Station (USDA) and composed of a metal frame with a winch attached

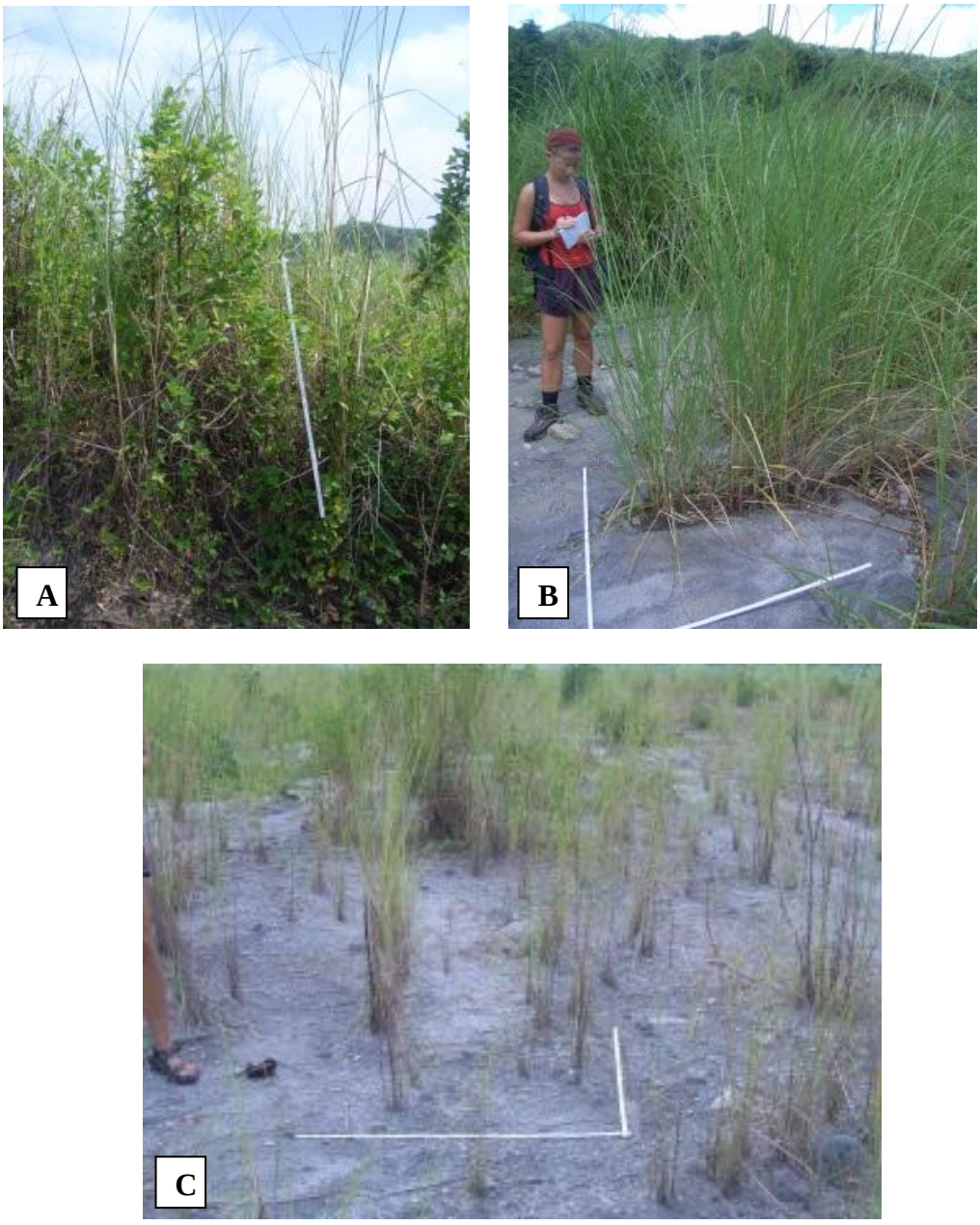

Figure 4-1. Vegetation on the braidplain exists in three growth patterns: (A) dense, (B) clumpy, and (C) sparse. Vegetation 1x1 meter plots were set up to collect data on each vegetation type and growth pattern. In each plot data collected were comprised of substrate type, species type, stem count, stem diameter, stem height, and percent cover.

to a load cell and displacement transducer and a data logger (Figure 4-2). Different size roots were attached to the load cell and displacement transducer using u bolts of various sizes. The winch was then cranked at steady rate until the roots broke (Pollen and Simon, 2005). Root diameter and tensile strength measurements were recorded. Only roots belonging to the grass *Saccharum spontaneum*, the dominant species at both field sites, were tested (Figure 4-2). Where roots were tested, surface sediment samples were taken and vegetation height and stem diameter were recorded.

Root density data were collected to quantify the roots of specific plant species (Figure 4-3). Single plant samples of *Saccharum spontaneum* and *Parasponia Rugosa* were isolated and then a root sampler, of a known volume, was placed 10 cm away from the main stem of the plant. Samples were taken by excavating the cylindrical sample. Samples were then dried, roots removed from sediment, and roots were weighed. Vegetation diameter and height were recorded to compare vegetation size with root density.

Because vegetation can trap fine sediment from travelling downstream (Brookes et al., 2000; Gran and Paola, 2001; Easson and Yarhrough, 2002; Tal et al., 2004; Wynn et al., 2004; Tal and Paola, 2007; De Baets et al., 2008) surface samples were analyzed for sand, silt and clay percentages. Sediment samples were taken from vegetation plots and root strength sites. These samples were analyzed using a hydrometer to determine sand, silt and clay percentages.

The second data set was collected to describe the channel dynamics (Figure 4-4). Movement of the braidplain was highly variable, so to quantify this rate of movement, daily photographs from two vantage points both on the Pasig-Potrero and Sacobia rivers were set up. The goal was to capture photographs of the rivers at 1-2 sites in the vegetated and non-vegetated portions of the channel over a 30-day period in August 2009. These images were then masked to distinguish areas of flow in the braidplain. Channel lateral migration rates were then calculated for both vegetated and non-vegetated portions of the braidplain.

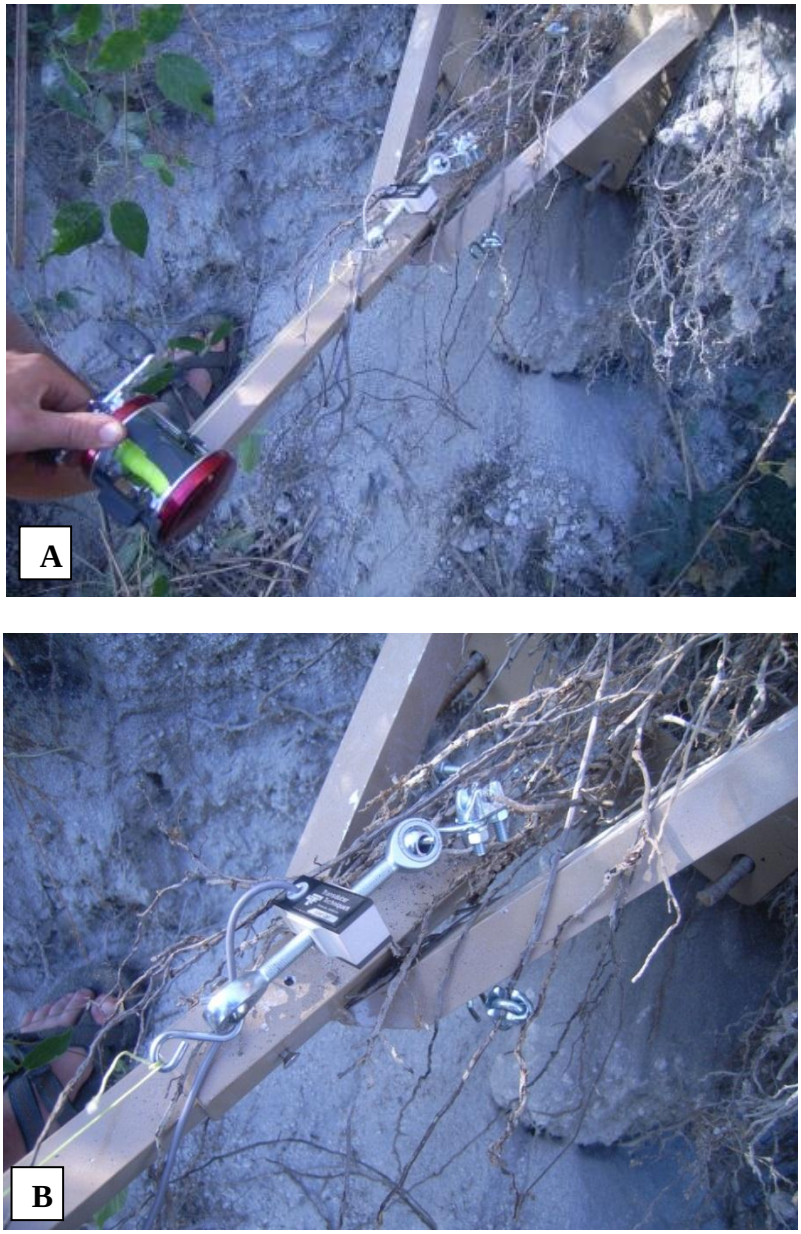

Figure 4-2. Root tensile strength and stress displacements were measured using a device called a Root-Puller. This device was composed of a metal frame with a winch attached to a load cell and displacement transducer and a data logger. Different size roots were attached to the load cell and displacement transducer using u bolts of various sizes. The winch was then cranked at steady rate until the roots broke. Only roots belonging to *Saccharum spontaneum*, the dominant grass at both field sites, were tested.

Figure 4-3. Root density data were collected on various sizes of *Saccharum spontaneum* and *Parasponia rugosa.* These data were used in obtaining values for the added cohesion to the soil matrix provided by root networks. (A) A single stem of *Saccharum spontaneum*, an example of a stem that was tested for root.

4.2. ANALYZING FIELD DATA

To determine how much additional cohesion was added due to roots the Pollen and Simon (2005) RipRoot model was utilized. The RipRoot model is part of a larger physically-based model, BSTEM (Bank Stability and Toe Erosion Model) (Simon et al., 2000), which simulates shear-type bank failure that occurs when the driving force exceeds the resisting force (Simon et al., 2000; Simon and Collison, 2002; Pollen-Bankhead and Simon, 2009). BSTEM calculates the Factor of Safety (F_s) of the bank by looking at two processes: the failure by shearing of a soil block of variable geometry; and 2) the erosion by flow of bank and bank toe material. The model allows one to input field data on bank geometry as well as the material composition of the bank. The model output, F_s, provides a measure of the bank stability. The bank is said to be 'stable' if F_s is greater than 1.3. Banks with a F_s value between 1.0 and 1.3 are said to be 'conditionally stable' while banks with a F_s value less than 1.0 are 'unstable' (Simon et al., 2000).

RipRoot allows one to input field data to calculate additional cohesion due to roots. Input variables include the number and size of roots present on a 1 square meter bank and the general tensile strength – root diameter relationship, developed from root strength data. The model acts as a progressive failure and then redistributes stress equally to each root. The number of roots for each vegetation growth class (dense, clumpy, and sparse) was determined by using the average stem count for each growth class in the 1 square meter plots and dividing it by 10, to examine the inner 10 cm of bank. Using root density measurements, the average number of roots for different sizes (using height measurements) of vegetation was established. This produced values of root count for a 1 m^2 bank to input into RipRoot. Values for the tensile strength – root diameter relationship were obtained through root strength field data. The model acts as a progressive failure model, as roots break the remaining stress is redistributed equally to each remaining intact root. The output of the RipRoot model is an estimation of the

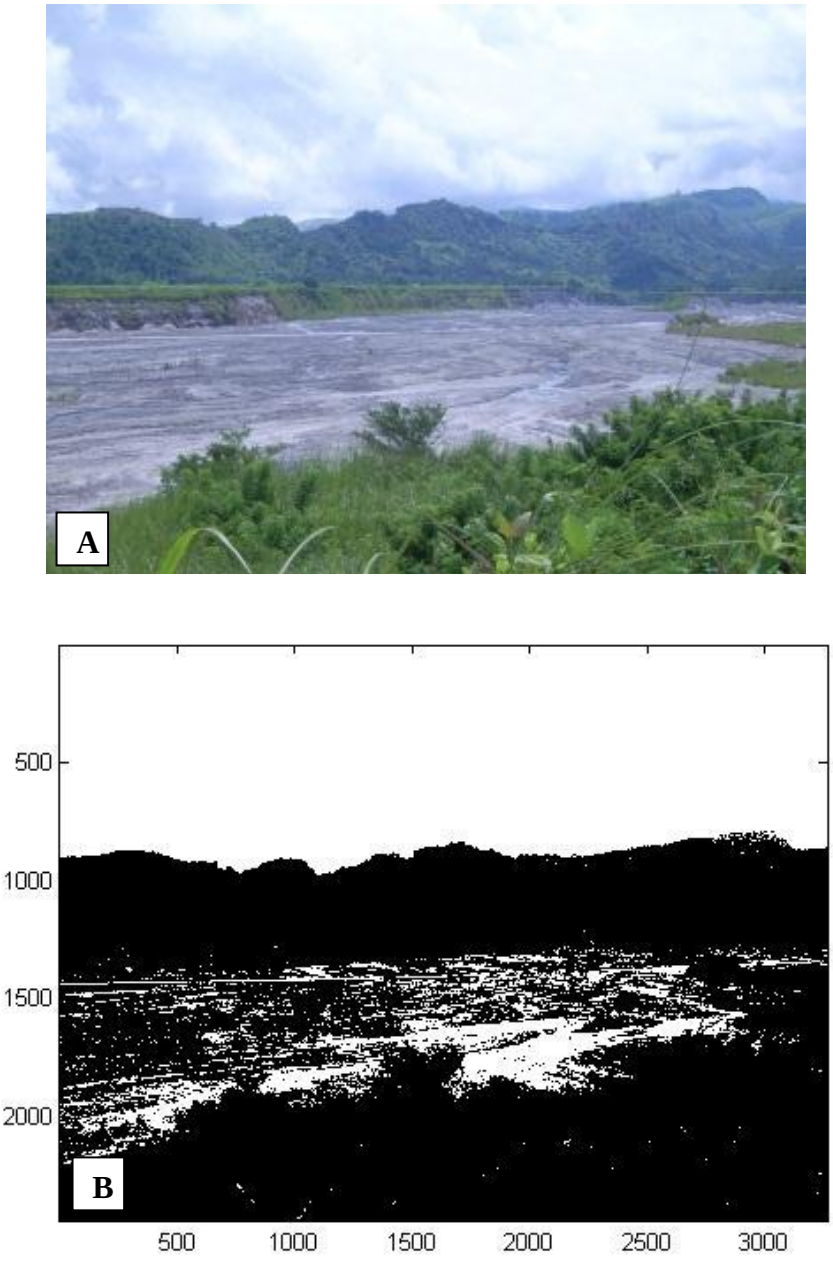

Figure 4-4. (A) Channel migration photos were taken daily at three vantage points above the river. These data were used to compare daily migration rates of the braidplain in vegetated and non-vegetated areas. (B) Daily photos were then turned into thresholded black and white images to track the movement of flow across the braidplain. Thresholding the image allows one to easily distinguish between areas of flow and channel bed on the braidplain.

cohesion (MPa) that is added to the shear strength of the soil. This, in turn, was added to BSTEM to determine what the effect of the added cohesion would be on a bank composed of cohesionless sand and gravel.

4.3. NUMERICAL MODELING

Vegetation has numerous effects on braided channels: vegetation corrals flow, it traps fine-grained sediment, roots strengthen the channel bed and banks making erosion more difficult and stems reduce and re-route flow. To explore how vegetation affects braided rivers in an aggrading system like at Pinatubo, a model was developed that focused on the two fundamental components of vegetation: roughness which affects water velocity, and cohesion which makes erosion more difficult. We used a reduced complexity model to explore the relationship between vegetation and channel dynamics.

A simplified version of the Murray and Paola (2003) model was created to examine the relationship between vegetation and channel dynamics. A 200 x 42 cellular matrix was constructed to initialize the landscape. One matrix was created to track flow (Q matrix), while another matrix was constructed to track bed elevation changes (Z matrix). In each cell in the matrix bed elevation along with water and sediment discharge were tracked, in dimensionless units. First the bed was given a 2% slope, to mimic the conditions at Mount Pinatubo. In addition, on the bed, random white noise perturbations three orders of magnitude less than the slope were introduced to give the bed topography. High banks of 1 cell in width on the sides of the matrix prevented lateral migration beyond the modeling domain. An iteration of the model begins at the first row with water being introduced to the matrix carrying sediment. Water is routed through the grid and ensuing sediment transport rates are determined. At the end of each timestep, elevation of each cell is then adjusted, based on mass conservation, according to the difference between the total sediment loads entering and leaving the cells.

An iteration of the model begins with water, Q, being introduced to the uphill end of the middle six cells,Q. To initiate water discharge, water in one cell was routed to two of three possible downhill neighbor cells. Water was routed into the two cells with the steepest slope. The amount of water going to each of the cells, Q_{wi}, was determined by the slope of those cells (S_i), by the equation:

$$Q_{wi} = Q_0 S_i / \sum S_i \quad (13)$$

where Q_{wi} is the water discharge andS_i is the slope between the cells. This unconstrained flow of water self-organized into a braided channel pattern.

Second, sediment was introduced into the matrix, determined by a stream power index with the amount of sediment moving through the system directly correlated to water discharge and cell slope. The following equation was used to route sediment:

$$Q_s = \beta\ Q_w S_i \quad (14)$$

where Q_{si} is the amount of sediment in motion to each cell and β is a constant of proportionality, equal to 0.8 in default model runs (Figure 4-5).

Vegetation was the last step added to the model. Vegetation was treated as an impedance to sediment transport, thus incorporated into a term K that is essentially a function of the strength of the vegetation which, in turn, is a function of the vegetation age. This effect of vegetation, shown as a decrease in sediment transport, is shown by the equation:

$$Q_s = (\beta\ Q_w S_i\ ) - \alpha K \quad (15)$$

where α (0.001 in default model runs) is a constant of proportionality and K the vegetation variable, which can be thought of as representative of vegetation

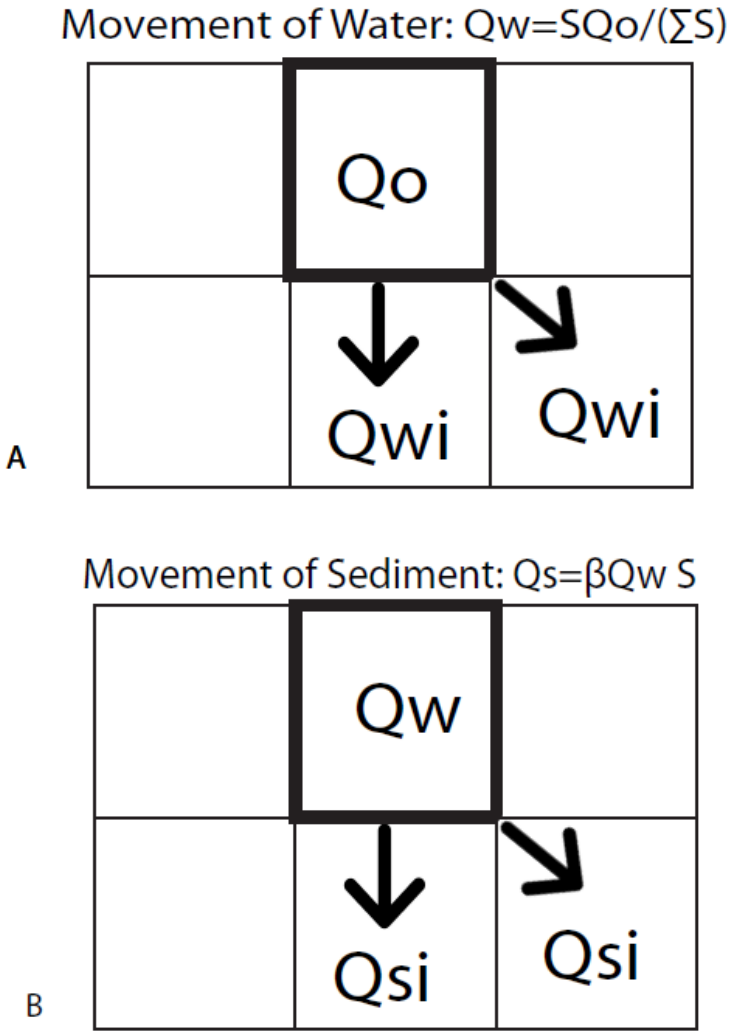

Figure 4-5. (A) Water was routed through the cellular lattice based on slope. To initate water discharge, water in one cell was routed to two of three possible downhill neighbor cells based on which two had the greatest downhill slope. The amount of water going into the cells, Q_w, was determined by the slope of the cells using the equation: $Q_{wi} = Q_0 S_i / \sum S_i$. (B) Sediment was routed through the cellular lattice based on the stream power index, as the amount of sediment moving through the system is direcly correlated to the water discharge and slope between cells following the equation: $Q_s = \beta Q_{wi} S_i$.

history. K does not start affecting sediment transport until the braidplain has become established, after a lag time of 50 timesteps. After the lag time vegetation begins to affect sediment transport. Vegetation occurs initially in areas of no flow or sediment and grows over time. This is accomplished in the model by recording the time since a cell has been vacant of sediment and water flow, as that time increases so does the vegetation in that cell, and subsequently the surrounding cells. This time counter can be reset back to zero if sediment is transported into a cell at later time steps, analogous to the vegetation being wiped out. As vegetation continues to grow in a cell it decreases sediment transport in that area and has a colonizing effect. The model is then run to allow flow, sediment, and vegetation to interact.

To track the changes in vegetation growth patterns and the interaction of vegetation and the braidplain several model scenarios were run to explore the fundamental conditions occurring at the Pasig-Potrero and Sacobia braidplains. Field observations reveal that vegetation growth density and sediment aggradation are major factors in the interaction of vegetation and channel dynamics. First, varying α, the constant of proportionality of K, is analogous to varying vegetation growth density. Values for α in model runs were 0.0001. 0.001. 0.01, 0.1, and 1.0. The order of magnitude variation of α correspond to stem count data from field measurements which range from 1 to 1000, values range from single stem grasses to dense vegetated areas. Second, varying the model coefficient (β) allowed the effect of fluvial diffusivity on the system to be examined as a proxy for sediment flux. Values for β in model runs were: 0.5, 0.8, 1, 1.5, and 3. Values of β allow one to explore the order of magnitude changes in flux which has affected aggradation rates in the braidplain post-eruption. To examine the effects of the tested variables, model runs were carried out for five different variable values, for each tested variable. The total number of wet cells was recorded and divided by the model length (200 cells) to produce the term w^*, which can be

used to compare channel width in model runs. Matlab code used is located in Appendix B.

5.0 RESULTS

5.1. FIELD RESULTS

As the complex interplay of vegetation and fluvial systems is readily recognized, better defining this relationship is crucial to better understanding it. The Pasig-Potrero and Sacobia rivers provided two sites to study the interplay of a braided channel and vegetation in an active aggradational system. By quantifying the effects of vegetation locally, using field data, prediction as to the trajectory of channel migration and evolution can be hypothesized for different growth scenarios in braided systems. Local vegetation effects on the braidplain include increased roughness affecting the flow velocity and increased cohesion, making erosion more difficult.

5.1.1. CHANNEL PLANFORM

The eruption of Mount Pinatubo in June of 1991 deposited 5-6 cubic kilometers of pyroclastic flow deposits onto the flanks of the volcano, contributing a large influx of loose sediment into the fluvial system. This caused the once meandering channels to become highly active aggrading braided systems. As a result, the Pasig-Potrero and Sacobia rivers experience high sediment transport rates (Hayes et al., 2003; Gran et al., 2006), especially during the rainy season. This caused the braidplains to aggrade rapidly through time, at a rate of 5 meters/year in 1997, decreasing to 0.7 meters/year from 2002-2009 (Gran et al., 2011) (Figure 5-1).

The Pasig-Potrero and Sacobia braidplains drain the east flank of Mount Pinatubo and range in width from 300-500 meters. The location of flow in these braided channels is highly variable and able to change at any time. On a cross-

section line there are 10-50 braids on average, of varying sizes. Aerial photographs and cross-section field data reveal the size of the braids ranging from 0.1 meters to 20.0 meters in width (Figure 5-2). Grain size distribution data, from 52 Wolman pebble counts taken in 2009 and 2010, show that the composition of the braidplain is mainly sand and gravel. During the rainy season the composition of the active channel is 56% sand, 32% gravel, and 12% cobbles and boulders, with a D_{50} of less than 2 mm. The composition of the vegetated channel during the rainy season is 41% sand, 51% gravel, and 8% cobbles and boulders, with a D_{50} of 5.9 mm. During the dry season the braidplain becomes considerably coarser, in the active channel the braidplain composition is 3% sand, 48% gravel, 41% cobbles and boulders (Figure 5-3).

Field observations reveal unvegetated areas experience highly variable flow and fairly quick migration rates compared to vegetated areas. Aerial photographs show that the majority of the braidplain is unvegetated and that vegetation occupies 10-40% of the braidplain in a given area. Daily photographs taken for a 30-day period show that flow in the unvegetated region of the braidplain is more variable than flow in the vegetated region. In a 30-day period at the Pasig-Potrero the unvegetated channel occupied 60% of the braidplain while the vegetated channel occupied 40%. At the Sacobia the un-vegetated channel occupied 90% of the braidplain while the vegetated channel occupied 10%.

5.1.2. VEGETATION CHARACTERISTICS

Field observations reveal that vegetation does indeed constrain and help to organize flow on the braidplain. By gathering data on specific vegetation characteristics we attempt to explain, physically, how vegetation changes the morphology of the braidplain. This was accomplished through aerial mapping

Figure 5-1. The Pasig-Portero braidplain experiences high sediment transport rates, especially during the rainy season. As a result, this has caused the braidplain to aggrade rapidly through time, at a rate of 0.7 meters per year from 2002-2009 (Gran et al., 2011). (A) A bedrock knob on Pasig-Potrero at Hanging Sabo site approximatly 1 km north of Delta 5 in 1997 (image from Gran and Montgomery, 2005). (B) The same bedrock knob in August 2009.

Figure 5-2. This is an aerial image taken in August 2009 of the Pasig-Potrero braidplain at the Delta 5 site. The majority of the flow is concentrated on river right. Transect A to A' shows a distance of approximately 500 meters with a 5 meter drop in elevation. On an average cross section line there exist 10-50 braids of varying sizes. Field data reveal the size of the braids to range from 0.1 m to 10 m in width. The composition of the braidplain is mainly sand and gravel.

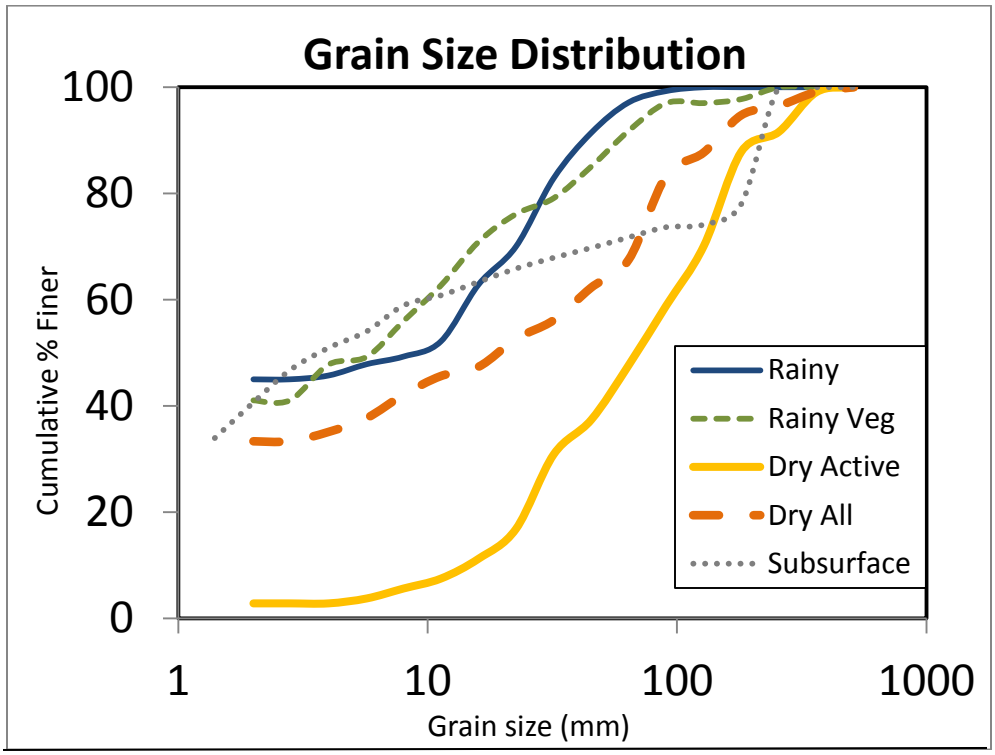

Figure 5-3. Pebble count data shown on a plot of grain size distribution on Pasig-Portero braidplain. The composition of the braidplain during the rainy season is similar in the vegetated and unvegetated areas, the latter being slightly coarser. During the dry season the composition of the braidplain is much coarser (Gran, in review).

and measurements of vegetation size and growth density. These data provide a base for calculations of added roughness and cohesion into the system.

Vegetation growth on the braidplain is made of up a mix of riparian species. The dominant vegetation species identified include grasses (*Saccharum spontaneum, Miscanthus floridulus, Phragmites karka,* and *Melinis repens*), vines (*Centrosema molle* and *Calopogonium mucunoides*), forbs (*Chromolena ordata*), and woody trees (*Parasponia Rugosa*). The presence of vines was minimal and hardly rooted to the soil matrix, its growth was mainly concentrated as a mess of thin vines amidst the upper meter of grasses. Woody trees were present in about half of the vegetation plots and varied in height from 0.5-1.55 meters. *Saccharum spontaneum,* relative of sugar cane, was the most common species present on the braidplain, composing about 85% of vegetation present, growing mainly in large clumps. Due to its overwhelming presence on the braidplain, data pertaining to *Saccharum spontaneum* provide a good representation of variations in vegetation growth and characteristics on the braidplain.

It is clear from aerial photographs that vegetation growth occurs in different patterns and densities on the braidplain (Figure 5-4 and Figure 5-5). In order to document the differences in growth patterns we set up a classification scheme in which areas of vegetation were classified as dense, sparse and clumpy. Dense and sparse vegetation represent the two end-members of vegetation growth and were differentiated by sight. For the most part, dense vegetation occurred as growth you could not see through, composing 70-100% of the vegetation plot area. Sparse vegetation was composed of a few solitary grass stems, composing 1-30% of the vegetation plot area. Clumpy vegetation was a mix of the two, usually a mix of *Saccharum spontaneum* and *Parasponia Rugosa,* growing in clumps, composing 30-70% of the vegetation plot.

To quantify the differences in each of these groupings, 76 1x1 m^2 vegetation plots were set up in which substrate type, species type, stem count, stem diameter, stem height, percent cover, and bed and bank strength using a

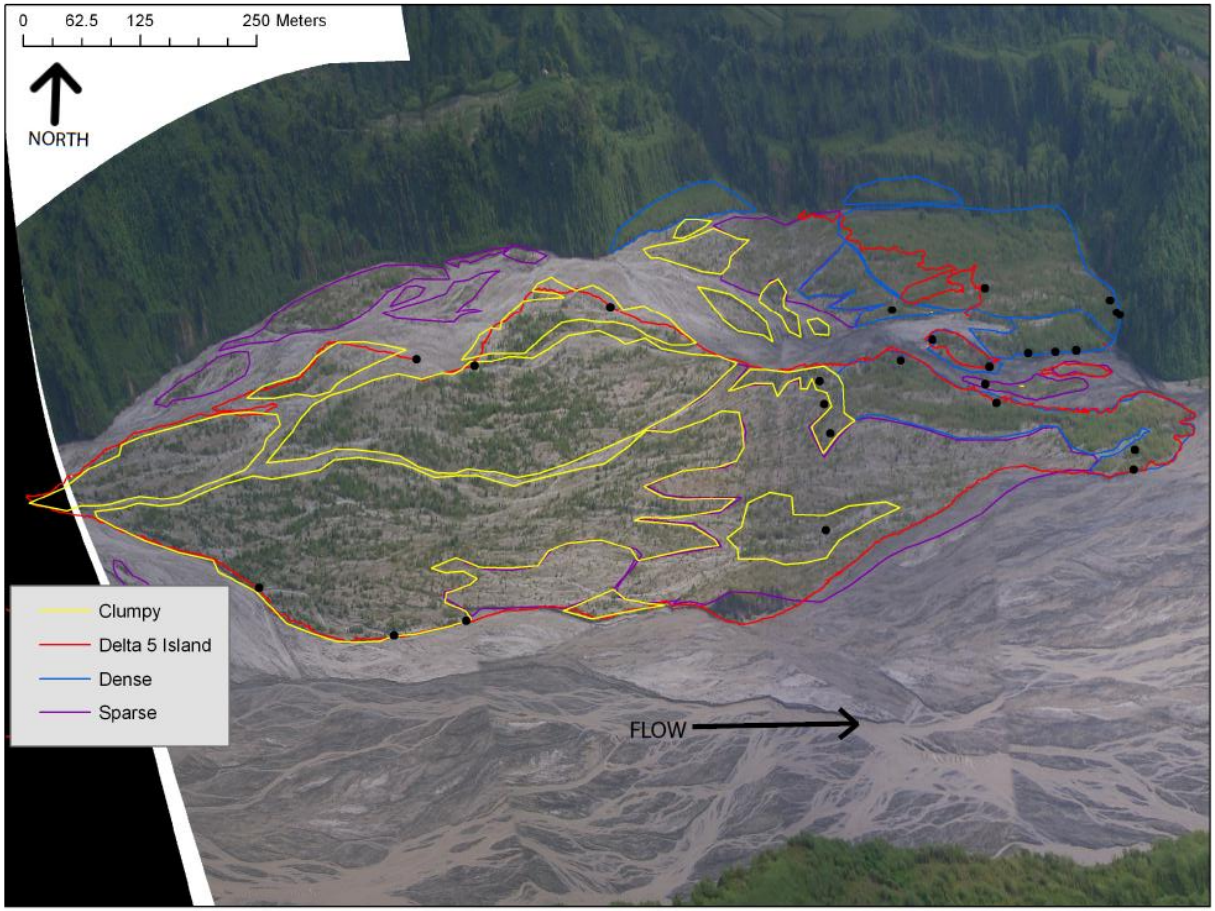

Figure 5-4. Aerial image of mapped vegetation patterns at the Pasig-Potrero braidplain at the Delta 5 site. From aerial photographs and vegetation plot data, vegetation growth patterns were categorized as dense, clumpy and sparse. At Delta 5 the majority of the vegetation is situated on river left. Black dots in image represent locations of vegetation plot data.

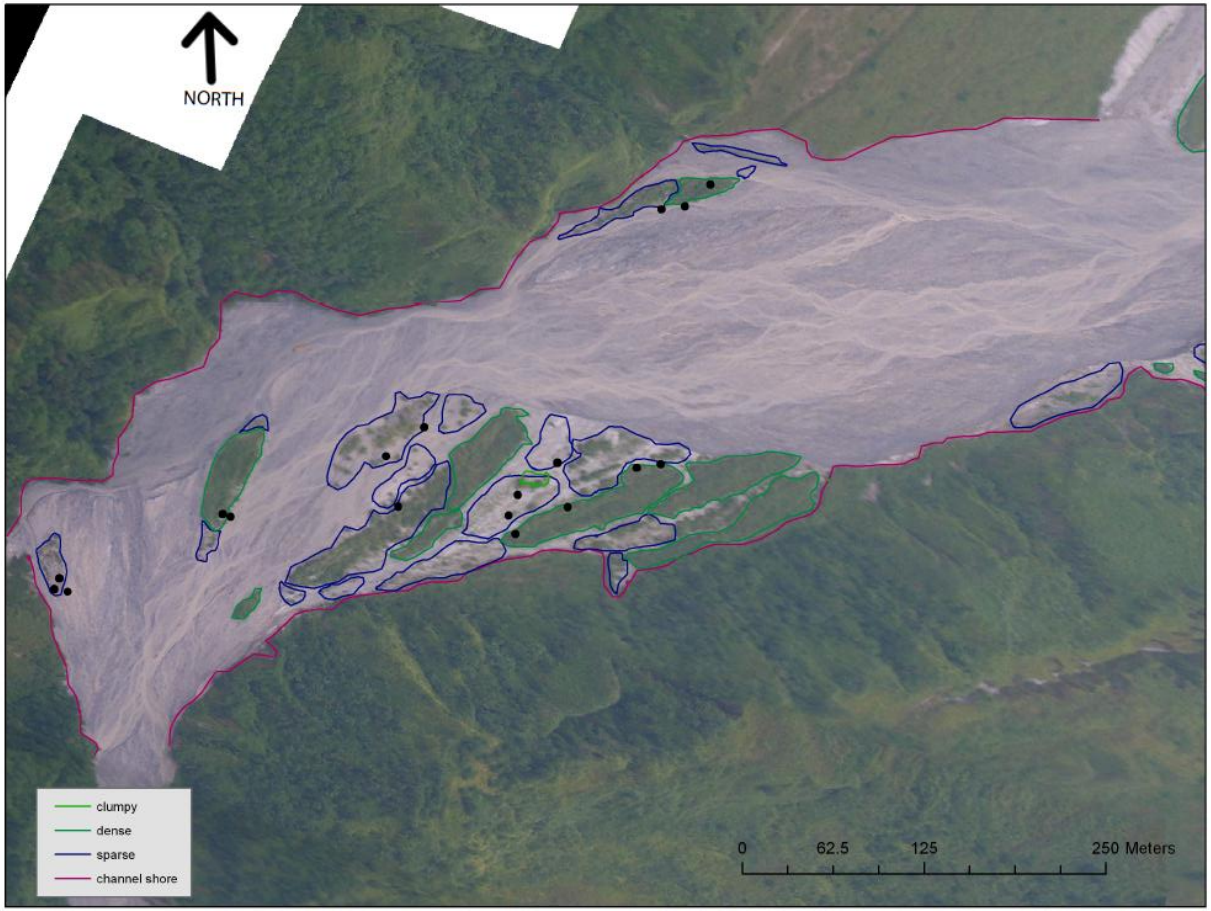

Figure 5-5. Aerial image of mapped vegetation patterns at the Sacobia braidplain. From aerial photographs and vegetation plot data, vegetation growth patterns were categorized as dense, clumpy and sparse. Black dots in image represent locations of vegetation plot data.

Torvane were recorded. The majority of vegetated banks were 0.5 – 1.5 meters tall. Twenty-seven dense vegetation plots, 20 clumpy vegetation plots, and 29 sparse vegetation plots provide data on the growth characteristics of vegetation on the braidplain, specifically *Saccharum spontaneum.*

Results from vegetation plots show changes in the size and growth density of *Saccharum spontaneum* in the study area. Dense vegetation plots had higher stem count, and on average, larger stem diameter and height, than sparse and clumpy vegetation plots. Dense plots had an average of 135 stems, while clumpy plots had an average of 40 stems and sparse plots had an average of 26 stems. *Saccharum spontaneum* in areas of dense vegetation vary from 1.32 – 2.44 meters tall with an average diameter of 9.92 mm, while the grass was found to be 0.72-1.42 meters tall with an average diameter of 5.25 mm in areas of sparse vegetation. Vegetation plot data are summarized in Table 5-1, and the full vegetation plot data set is available in Appendix C.

5.1.3. ROUGHNESS

One major effect vegetation has on the braidplain is increasing roughness. Roughness affects the velocity of flow in the channel. Vegetation enhances bed roughness by increasing flow resistance, therefore reducing flow velocity and increasing flow depth (Stone and Tao Shen, 2002; Liu et al., 2008). The degree to which flow velocity is affected is dependent on flow depth, area concentration of stems (number of stems per unit bed area), stem length, and stem diameter. Vegetation slows flow and helps it to organize itself into fewer channels that are narrower and deeper (Tal et al., 2004).

As vegetation density increases in the braidplain the roughness of the channel increases, thus decreasing the average channel velocity. The apparent channel velocity decreases with increased vegetation density, meaning water moving through a vegetated area moves slower than water through an un-

	Average Value			Variance		
	Dense	**Clumpy**	**Sparse**	**Dense**	**Clumpy**	**Sparse**
Number Plots	27	20	29	*nd*	*nd*	*nd*
Bank height (if present) (m)	0.44	0.52	0.72	0.003	0.07	0.10
Number Stems	135	40	26	17.99	10.21	8.23
Stem Diameter (mm)	9.92	6.23	5.25	5.52	15.74	14.494
Stem height (shortest) (m)	1.32	0.74	0.72	0.117	0.105	0.218
Stem height (tallest) (m)	2.44	1.53	1.42	0.335	0.344	0.411

nd = no data

Table 5-1. Seventy-six 1x1 meter vegetation plots were set up to collect data concerning vegetation characteristics. Data above summarize plot results for the grass *Saccharum spontaneum*, the dominant species present on the braidplain.

vegetated area. By treating vegetation as emergent cylinders in a flow (Stone and Tao Shen, 2002) with density and size as measured in the field, normalized velocities decrease to an estimated 88% of the main un-vegetated flow in dense vegetation growth. Flow velocity decreases to 96% in clumpy vegetation growth, and 97% in sparse vegetation growth.

5.1.4. COHESION

The other major effect vegetation has on the braidplain is increasing cohesion. Cohesion is added to the soil matrix by roots which physically bind soil particles together. Increased cohesion is shown to decrease sediment transport and induce the deposition of fine-grained cohesive sediment, which further increases cohesion (Tal et al., 2004; Pollen and Simon, 2005; De Baets et al., 2008). Increased cohesion makes erosion more difficult: as bank strength is increased, the critical shear stress (τ_c) required to begin eroding the bank increases (De Baets et. al., 2008; Abernathy and Rutherford, 2001; Liu et al., 2010; Wilson et al., 2003; Stoesser et al., 2009).

To analyze the influence of vegetation on cohesion, measurements were made in the field of root size, strength, and density. Roots of larger (larger height and diameter) *Saccharin spontaneum* grow more densely than that of smaller *Saccharin spontaneum*. Roots of dense *Saccharin spontaneum* grow in a density of 8.27 x 10^{-4} g/cm^3. Roots of clumpy *Saccharin spontaneum* grow in a density of 1.0 x 10^{-4} g/cm^{3}and sparse in a density of 2.5 x 10^{-5} g/cm^3(Appendix D). Root density data were obtained from field measurements. Root density measurements along with average stem count data from field data, were combined to obtain root count values for 1 square meter of bank face, for each vegetation growth class. The average number of roots per unit area for each vegetation growth class varies by orders of magnitude (dense: 2000-3000 roots/m^2 of bank face, clumpy: 320-480 roots/m^2 of bank face, sparse: 30-70 roots /m^2 of bank face.

The majority of sediment present on the braidplain is sand. However, areas of dense vegetation have slightly higher silt and clay percentages than their sparser counterparts. Sand/silt/clay ratios in areas of dense vegetation average 75/23/2, in clumpy vegetation average 92/7/1, and in sparse vegetation average 94/6/0. Thus, dense vegetation has a higher percentage of fine-grained sediment than sparser vegetation.

Root strength was tested for 181 roots of various sizes using a Root Puller Device. Roots of smaller diameter have a higher tensile strength than roots of larger diameters (Figure 5-6). On average roots varied from 0.1 – 2.5 mm in diameter. The tensile strength of root with diameter 0.1 – 0.5 mm varied from 10 – 250 MPa, based on 78 root measurements. The tensile strength of medium sized roots, with diameter 0.5 – 1.5 mm, decreased to 10- 60 MPa, using 66 root measurements. The largest roots, with diameter 1.5 – 2.0 mm had the lowest tensile strengths, ranging from 10-25 MPa, based on 37 root measurements (Appendix E). This relationship holds with previous studies (Pollen and Simon, 2005; De Baets et al., 2007). Using these field data the root tensile strength – diameter relationship for *Saccharin spontaneum* was established to be: $T_r = 10.21d^{-1.211}$ using the Pollen and Simon (2005) system.

Root measurements along with channel geometry data were input into BSTEM (Simon et al., 2000; Simon and Collision, 2002) and RipRoot (Pollen and Simon, 2005) to assess how roots affect cohesion and bank stability (Table 5-2). Values input into RipRoot were obtained using the root tensile strength – diameter relationship for *Saccharin spontaneum* (Table 5-3). In addition, root counts for a one square meter of bank face were input. As mentioned previously, the number of roots present on a given bank face vary for dense, clumpy and sparse vegetation plots due to plant growth density and size.

BSTEM and RipRoot model results show that vegetation adds cohesion to a soil matrix and that bank stability is increased in the presence of vegetation (Table 5-4). Un-vegetated, unstable banks become stable even with the smallest

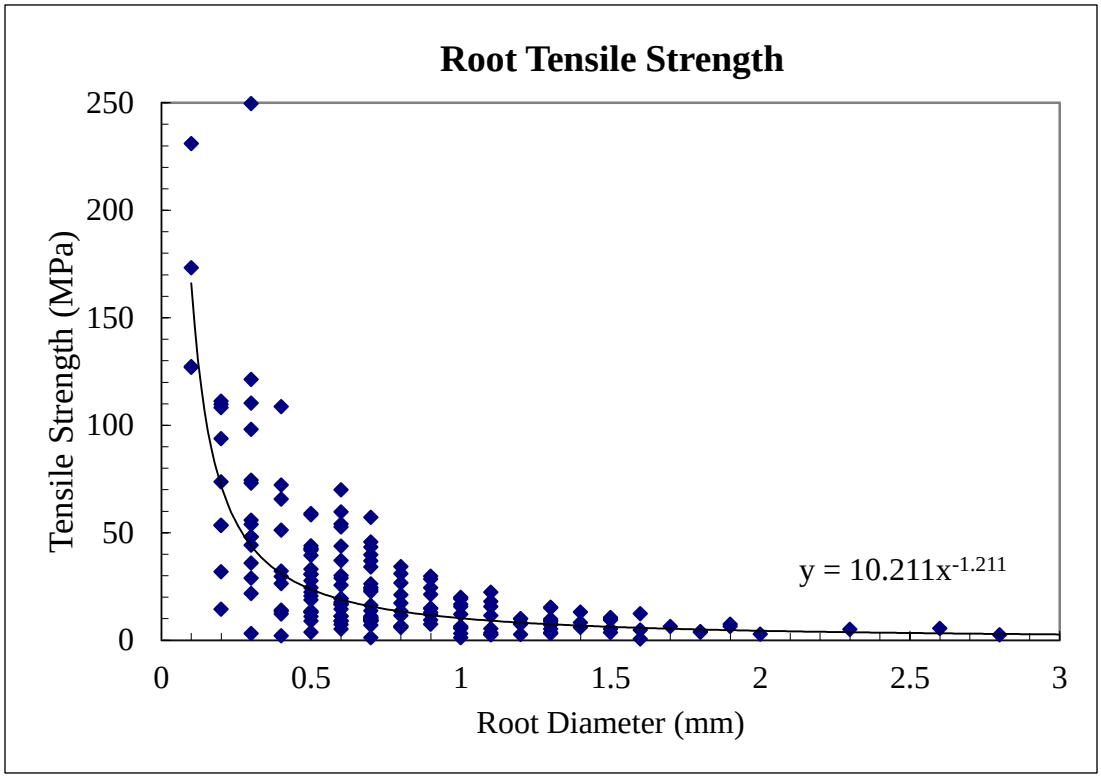

Figure 5-6. One hundred and eighty-one roots were tested for their tensile strength using the Root Puller device. Field data results show that root tensile strength decreases with increasing root diameter. Root tensile strength data waere used to obtain values for additional cohesion that roots add to the soil matrix.

BSTEM Input Data

Input Geometry	
Input Bank Height (m)	1.00
Input Bank Angle (degrees)	80.00
Input Bank Toe Length (m)	0.00
Input Bank Toe Angle (degrees)	0.00
Input shear surface angle (degrees)	40.00
Bank Layer Thickness	
Layer 1 (m)	0.20
Layer 2 (m)	0.20
Layer 3 (m)	0.20
Layer 4 (m)	0.20
Layer 5 (m)	0.20
Channel Flow Parameters	
Input reach length (m)	100.00
Input reach slope (m/m)	0.02
Input elevation of flow (m)	0.10
Input duration of flow (hrs)	100.00
Input Bank Material	
Layer 1	fine rounded sand
Layer 2	fine rounded sand
Layer 3	fine rounded sand
Layer 4	fine rounded sand
Layer 5	fine rounded sand
Bank Toe Material	fine rounded sand
Non-cohesive particle diameter (mm)	1.00
Critical Shear Stress (Pa)	0.71
Erodibility Coefficient (cm3/Ns)	0.12

Table 5-2. Table of data input into the BSTEM Model (Simon et al., 2000). Input data are based on field data.

RipRoot Input Data

Bank Vegetation and Protection *(choose own tensile strength parameters)*	
Coefficient for root diameter curve	-1.211
Root tensile strength (MPa)	10.211
Dense Vegetation	--
Diameter class 0-1 mm	1500-2000
Diameter class 1-2 mm	500-1000
Clumpy Vegetation	--
Diameter class 0-1 mm	280-400
Diameter class 1-2 mm	40-80
Sparse Vegetation	--
Diameter class 0-1 mm	20-60
Diameter class 1-2 mm	10-20

Table 5-3. Table of data input into the RipRoot Model (Pollen and Simon, 2005). Input data were compiled from field data. Tensile strength parameter data were compiled form root strength measurements. Root count data were compiled from root density and vegetation plot data.

amount of vegetation (added cohesion). Additional cohesion due to roots varies from 0.13 - 0.29 kPa in sparse vegetation to 8.21 - 12.31 kPa in dense vegetation. BSTEM uses the Factor of Safety (F_s) term to compare stability of banks. Results from BSTEM show that this additional cohesion adds stability to the banks. Banks without vegetation present have a F_s value less than 1, showing instability. For the same bank geometry, the F_s value increases to stable values with the smallest amount of added cohesion. Sparse vegetation increases F_s to 1.46-1.47 while dense vegetation increases F_s to 2.11 - 2.51.

5.2. MODEL RESULTS

As it is recognized that the natural world has, in itself, many variables; a modeling approach that incorporates only the most important variables necessary to model fundamental behavior of the system is useful for distilling the real-world down to key processes. This was accomplished through a cellular modeling approach in which water and sediment were routed through a cellular lattice based on slope. Vegetation was then added to the lattice, as an impedance to sediment transport, or increased bank strength, using the approach of Murray and Paola (2003). Model results confirm the hypothesis that vegetation acts as a primary control on river morphology.

Initially, the cellular lattice existed as a highly mobile braidplain in which unorganized flow was routed over a cohesionless landscape. As sediment was fed into the system to simulate aggradation, an increase in the width of the braidplain and braiding intensity occurred. After introduction of the effects of vegetation to the cellular matrix the flow became organized (fewer channels that are narrower and deeper), reaffirming that the simplified approach of vegetation in the model does indeed capture the fundamental relationship between vegetation channel dynamics (Figure 5-7).

BSTEM and RipRoot Model Results

	Dense	Clumpy	Sparse
Added cohesion due to roots (kPa)	8.21-12.31	1.5-1.65	0.13-0.29
Fs (with vegetation)	2.11-2.51 (stable)	2.0-2.5 (stable)	1.46-1.47 (stable)
Fs (no vegetation)	0.8 (unstable)	0.8 (unstable)	0.8 (unstable)

Table 5-4. Table of results obtained from BSTEM (Simon et al., 2000) and RipRoot (Pollen and Simon, 2005). The same bank geometry was used for every model run; only the cohesion due to roots was changed. The value F_s refers to "Factor of Safety", a term used to compare the stability of banks. The bank is said to be 'stable' if F_s is greater than 1.3. Banks with F_s values between 1.0-1.3 are said to be 'conditionally stable', while banks with F_s values less than 1.0 are 'unstable'. When bank geometry values representative of Mount Pinatubo are input into BSTEM, the unvegetated banks are said to be unstable. The banks become stable with even the smallest amount of cohesion, as seen in the addition of sparse vegetation.

5.2.1. MODEL RUN RESULTS

Similar relationships were found in both field and model results relating vegetation and braiding intensity, channel morphology and mobility. Model runs were carried out to test the relationship between vegetation and braidplain morphology. Model runs include: 1) varying the vegetation growth density (α) and 2) varying fluvial diffusivity in the system (β). To examine the effects of the tested variables, model runs were carried out for five different variable values, for each tested variable. The value w* was recorded (number of wet cells divided by model domain length), to measure changes in channel width. The models were all run for the same amount of timesteps (10,000).

First, the effect of varying vegetation growth density was examined by varying the model variable α (Table 5-5). This can also be thought of as looking at changes in bank strength, as denser vegetation growth should have a higher amount of added cohesion than sparser vegetation growth. Field data support this observation; RipRoot results show that denser vegetation adds more cohesion to banks than sparse vegetation. As vegetation growth density increased so did its impedance to sediment transport. Model results show that as vegetation growth density increased w* decreased, leading to fewer, narrower, deeper channels (Figure 5-8). When α was 0.0001, representing the effects of single stems, w* had an average value of 13.71. While α was 1.0, representative of dense vegetation, w* was 7.31. Runs with the highest vegetation density produced channels with characteristics similar to single-thread channels.

Varying the degree of fluvial diffusivity in the system affects the ability for vegetation to sustain growth in the channel. This was examined by varying β (Table 5-6). Model results show that higher fluvial diffusivity in the system results in sustained braiding in the channel. When β was 3.0, representing a high ease of sediment redistribution in the system, w* had an average value of 27.84. When β was equal to 0.5, representative of a low ease of sediment redistribution

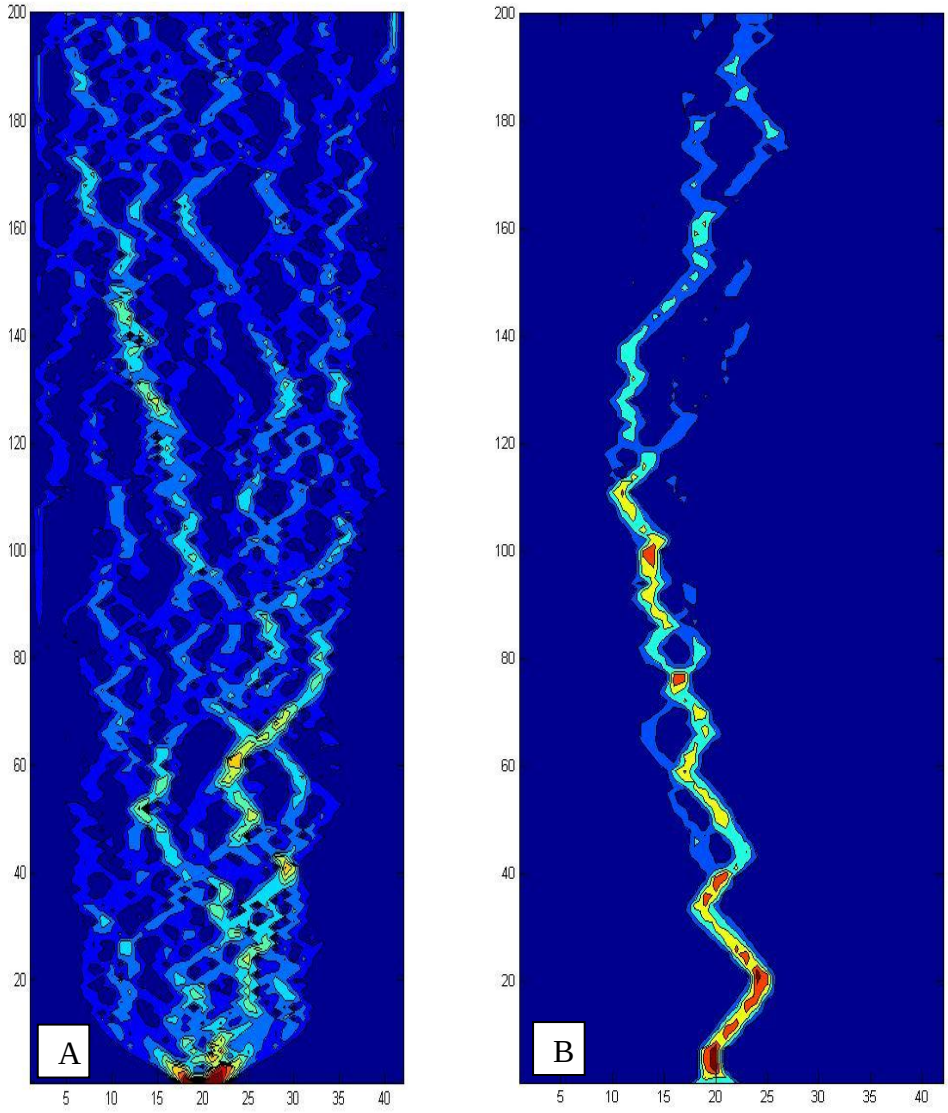

Figure 5-7. (A) Plot of flow (Q) for model results of flow and sediment routed over cellular lattice based on slope. Here, you can see how the routing of water over a cohesion-less bed creates a braided channel pattern. (B) Plot of flow (Q) for model results of flow and sediment routed over cellular lattice with the added effect of vegetation as an impedance to sediment transport. The flow has become organized into fewer active channels. Flow is from bottom to top.

Varying α (Vegetation Growth Density)

	α	w*	w* Std. Dev.	n
No veg	0	29	+/- 2.61	10
α 1	0.0001	13.71	+/- 1.57	35
α 2	0.001	12.78	+/- 0.75	35
α 3	0.01	11.99	+/-1.67	35
α 4	0.1	8.78	+/- 1.75	35
α 5	1.0	7.31	+/- 1.37	35

Table 5-5. Table of model results from varying vegetation growth density (α). Smaller α values correspond to single stems while large α values correspond to dense vegetation. Results show that with increasing vegetation density w* decreases, signaling smaller channel widths. The value n is the total number of model runs.

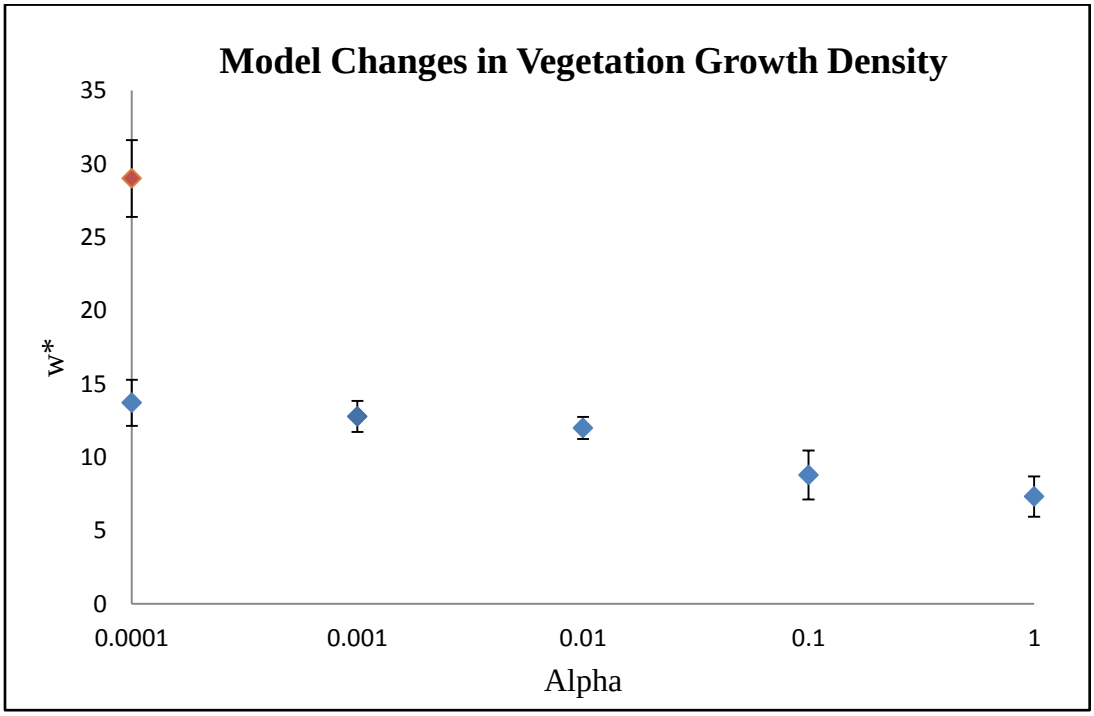

Figure 5-8. Plot showing model results for changing α. Results show that for higher vegetation growth densities (higher α) the total channel width decreases. The red value corresponds to model results without the effects of vegetation.

Varying β (Fluvial Diffusivity)

	β	w*	w* Std. Dev.	n
No veg	0.8	29	+/- 2.61	10
β 1	0.5	15.33	+/- 1.93	35
β 2	0.8	17.21	+/- 1.41	35
β 3	1	18.25	+/- 1.19	35
β 4	1.5	22.69	+/- 1.3	35
β 5	3	27.84	+/- 3.21	35

Table 5-6. Table of model results from varying fluvial diffusivity in the system, by varying the value β. Large β values represent a high ease of sediment redistribution in the system while low β values represent a low ease of sediment redistribution in the system. Results show that higher fluvial diffusivity rates cause braiding to sustain in the system through the model run. The value n refers to the number of model runs.

in the system, w* was 15.33. This shows that when fluvial diffusivity in the system decreases the channel has smaller widths (Figure 5-9).

Model results show that as vegetation cover increases channels become narrower and deeper, with fewer active channels along a cross-section. Cross-sections of the initial model conditions, in a braided state, show the braidplain to have 8-12 active channels with relatively small depths. When the model is continued to run to allow for the effect of vegetation the number of active channel decreases to 1-2 deep active channels (Figure 5-10).

6.0 DISCUSSION

Field and model results support the hypothesis that vegetation is having an effect on channel morphology at Mount Pinatubo. Field data from root strength and density measurements show that roots provide cohesion, increasing bank strength and decreasing erosion. Field data from vegetation plots show that channel roughness is higher in areas of higher vegetation density. Increased roughness provides resistance to flow, decreasing the average channel velocity in areas of dense vegetation. In sparse vegetation the average channel flow is decreased by an estimated 3% and in dense vegetation by 12%. Model results confirm field data and the hypothesis that vegetation acts a primary control on river morphology. Model runs show that a braided channel pattern can evolve into a single thread channel through the stabilization effects of vegetation. Model results show that after the effects of vegetation are allowed to occur the unorganized flow that characterizes braided rivers becomes organized into fewer, deeper active channels.

6.1. CHANNEL MOBILITY

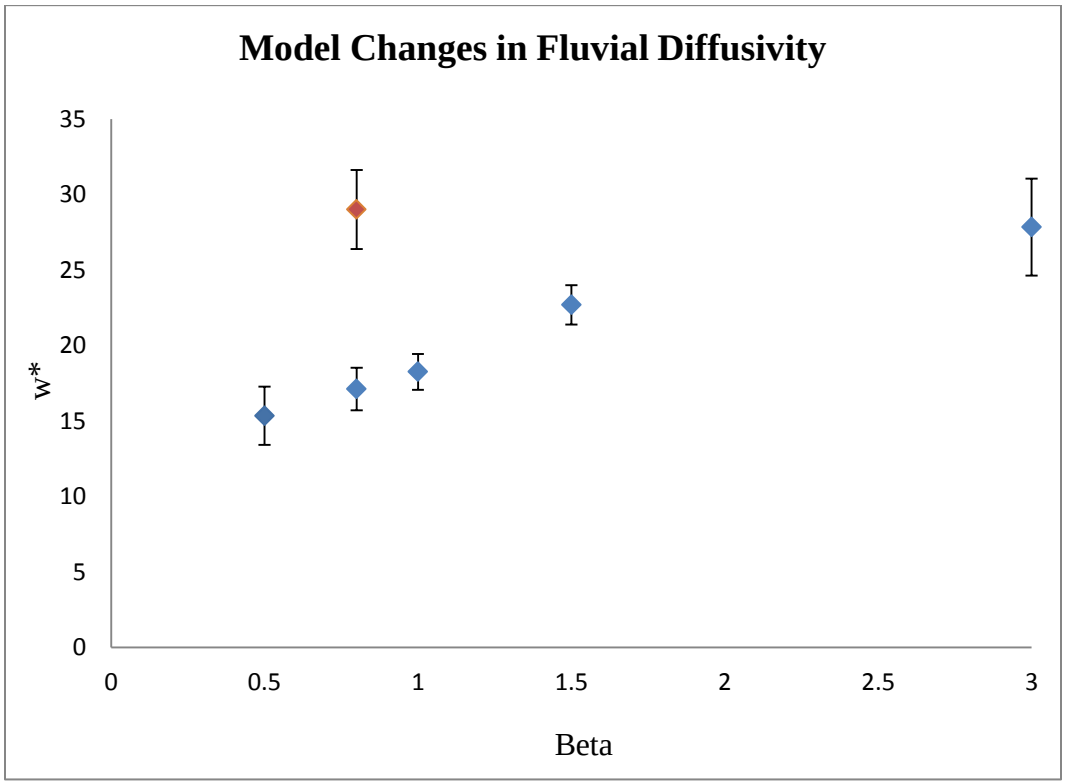

Figure 5-9. Plot showing model results for changing (β), which is fluvial diffusivity. Results show that for higher diffusivity rates (higher β) the channels remain more braided through time. The red value corresponds to model results run without the effects of vegetation.

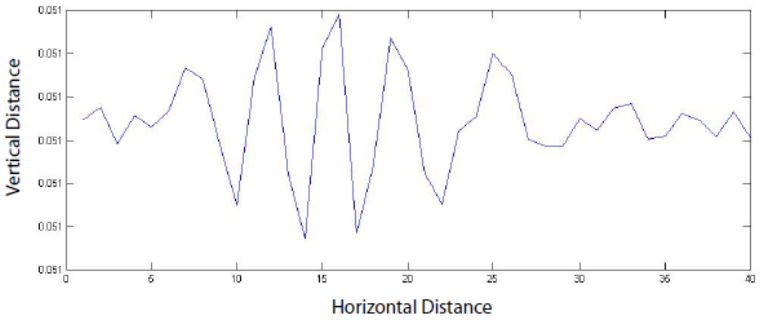

A. Cross-section through channel without effects of vegetation

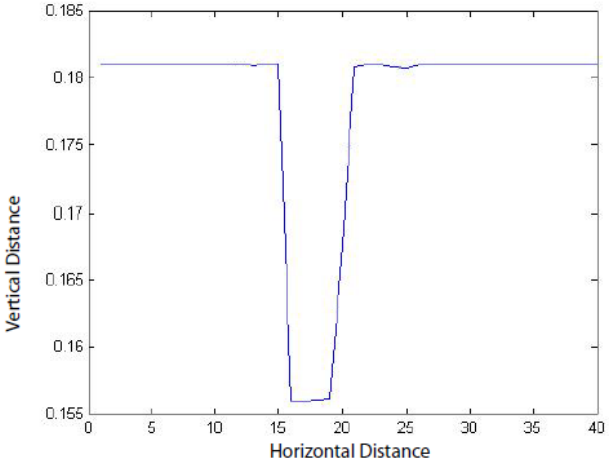

B. Cross-section through channel with effects of vegetation.

Figure 5-10. Channel cross-section plots. (A) Channel cross-section plot of braided channel, without the effects of vegetation. (B) Channel cross-section plot of channel with the effects of vegetation. Here it is visible that the vegetation is able to organize flow in the channel.

The Pasig-Potrero and Sacobia braidplains are highly mobile geomorphic features. These active braidplains have somewhat unpredictable behavior as their braids split, rejoin and migrate freely across their braidplains. It has been shown that vegetation is a primary control on this unstable behavior. Previous studies have shown that increasing vegetation, specifically along banks, decreases braiding intensity, channel mobility, and total channel width (Gran and Paola, 2001; Tal et al., 2004; Tal and Paola, 2007). Field data and model results agree with this finding and through this we are able to show that vegetation is having an effect on channel mobility at Mount Pinatubo.

Vegetation is affecting channel mobility through several different methods. Daily photographs and field observations during 2009 show that in a 30-day period flow in the vegetated regions of the braidplain is more constrained than flow in the un-vegetated regions. Vegetation increases channel resistance and provides resistance to flow. Vegetation adds cohesion to create stable banks that are more resistant to erosion. BSTEM and RipRoot results show that banks without vegetation are unstable with a F_s value of 0.8. Banks with even the sparsest amount of vegetation are considered stable, with F_s values of 1.46-2.25. Vegetation also constrains flow, corralling it into fewer, narrower channels with greater depths. Model results show that w* for an un-vegetated braidplain is 35-37.5 and 10-12 for a vegetated braidplain.

Although vegetation has survived through the rainy season for only a short period of time, its effects are clearly visible on the braidplain at Mount Pinatubo. Thus, better quantifying the relationship between channel dynamics and vegetation is fundamental to understanding braided river behavior.

6.2. Effects of Vegetation

Vegetation provides increased roughness to the braidplain by increasing channel resistance which in turn can affect flow velocity and channel geometry

(Gran and Paola, 2001; Tal et al., 2004; Tal and Paola, 2007). Field data calculations show that the apparent channel velocity decreases with increased vegetation density, meaning water moving through a vegetated area moves slower than water through an un-vegetated area. This interaction between flow and vegetation is shown to be a function of vegetation density and size as well as flow depth and velocity (Wilson et al., 2003; Stoesser et al., 2009; Liu et al., 2010).

Channels with higher roughness are shown to be more stable to fluctuations in sediment and water discharge (Gran and Paola, 2001; Tal et al., 2004; Tal and Paola, 2007). In the Pasig-Potrero and Sacobia braidplains this is seen as a reduction in the number of active channels. This is described by Tal et al., (2004) as the "corralling effect", in which vegetation is able to corral the flow into fewer, smaller channels that have smaller widths and greater depths, a key characteristic of single-thread channels. Model results support this observation, cross-sections taken from model data show that the average number of active channels in an un-vegetated braidplain is 14-16 while in a vegetated braidplain it is 1-2. With increased vegetation density the channel was able to organize itself to a single-thread pattern. As discharge in braided rivers is distributed over the entire width of the braidplain, it has been shown that blocking even a relatively small portion of that flow can lead to substantial decreases in channel width (Paola et al., 1999; Tal et al., 2004). In effect, vegetation helps not only to constrain the flow, but also helps to organize it (Tal et al., 2004).

Vegetation also increases cohesion in the braidplain which increases bank strength. Cohesion is added by root networks in the soil matrix, which add tensile strength. As roots within the soil physically help to bind particles together the bulk strength of the soil is increased. RipRoot results show that sparse vegetation adds 0.13-0.29 kPa of cohesion to the soil while dense vegetation adds 8.21-12.31 kPa. Moreover, these added amounts of cohesion are significant enough to create stable banks. BSTEM results show that the additional cohesion of even sparse

vegetation makes an otherwise unstable bank, stable. Thus, vegetation growth does not need to be dense to have a stabilizing influence on banks.

Increased bank stability is the main mode by which vegetation is represented in the cellular model. Model results support the conclusion that increased bank stability decreases the lateral mobility of channels and makes erosion more difficult. The degree of stability varies with vegetation density. Model results show that as you increase vegetation growth density channel width decreases (seen as a decrease in w*). Sparse vegetation ($\alpha = 0.0001$) gives an average w* value of 13.71 (+/- 1.57) while dense vegetation ($\alpha = 1.0$) outputs an average w* value of 7.31 (+/- 1.37). Denser vegetation leads to narrower, deeper channels. These data are supported by field results from Simon and Collision (2002), Tal et al (2004) and Wynn and Saied (2006) who found that by increasing bank strength, the critical shear stress (τ_c) necessary to erode sediment also increases. A higher critical shear stress can lead to an increase in bank angle can also help to allow narrower and deeper channels to develop.

6.3. Role of Aggradation

The ability of vegetation to corral and organize flow is very important, especially in aggradational systems such as the Pasig-Potrero and Sacobia braidplains. The constantly changing conditions during the rainy season, characterized by high sediment transport rates, make it difficult for vegetation to have the chance to take hold. Aggradation rates are high, but they have decreased through time from 5 meters/year to 0.7 meters/year over the last decade on the Pasig-Potrero (Gran et al., 2011). This decrease in aggradation rates has helped vegetation to take hold and persist through the rainy season when aggradation rates are at their highest.

The role of aggradation is especially important in the non-vegetated areas of the braidplains. Field observations reveal that while 40% of the Pasig-Potero braidplain is vegetated the majority of the active channel is located in the un-

vegetated portion (about 60%) of the braidplain. The non-vegetated portion of the braidplain is experiencing all of the active aggradation to the braidplain resulting in 5 meter elevation difference between the vegetated and un-vegetated portions of the channel. As this is evidence that vegetation is indeed stopping the migration of the active channel, it also suggests that the channel could begin to experience avulsions. This would most likely occur as the non-vegetated active channel continues to fill in, the channel would avulse rather than laterally migrate to fill in the elevation difference between the two areas.

Model results support these observations. High aggradation rates cause the channel to remain braided, as aggradation rates drop lateral migration is constrained as well as the number of active channels. Results show that w* values for low diffusivity, or times of low sediment yield, rates had an average value of 15.33 (+/- 1.93) and for high diffusivity, or times of high sediment yield, rates w* had an average value of 27.84 (+/- 3.21). This result helps explain behavior observed at the Pasig-Potrero and Sacobia braidplains, which have remained braided decades after the eruption. Results suggest that one explanation for this is that high sediment transport rates have not allowed vegetation to take hold. This supports the concept of a sediment yield threshold that must occur for vegetation growth to become established. At high sediment rates vegetation cannot sustain growth in the channel. When sediment yield decreases, vegetation is able to take hold and not be destroyed.

7.0 CONCLUSIONS

The effects of vegetation on the Pasig-Potrero and Sacobia braidplains are key to predicting their futures. Through field data collection and analysis as well as model results, several conclusions can be reached:

1) Vegetation decreases the lateral mobility of the braidplain and helps to create a smaller number of active channels that are narrower and deeper, thus decreasing braiding intensity and channel width.
2) A decrease in water and sediment discharge is important in allowing plants to grow and take hold. Once vegetation growth is established it is difficult to remove.
3) Vegetation helps to organize flow; it has a "corralling effect" in which it is able to coral the flow into fewer, smaller channels that have smaller widths and greater depths.
4) Vegetation growth contributes to decreasing the apparent channel velocity by providing resistance to flow.
5) Cohesion is added to the soil matrix through root networks as well as increased deposition of fine-grained, cohesive sediment. This cohesion increases bank strength, reducing stream bank erosion.
6) Even the sparse vegetation can have a profound influence on bank stability, contributing enough cohesion to stabilize banks.
7) The observed effects of vegetation on channel planform are consistent with fluvial effects that would move the braided to a meandering planform.

8.0 REFERENCES

Abernethy, B., and Rutherford, I.D., Where along a river's length will vegetation most effectively stabilise stream banks?, *Geomorphology,* 23, 55-75, 1998.

Abernathy, B., and Rutherford, I.D., The distribution of strength of riparian tree roots in relation to riverbank reinforcement, *Hydrological Processes,* 15, 63-79, 2001.

Abernathy, B., and Rutherford, I.D., The effect of riparian tree roots on the mass-stability of riverbanks, *Earth Surface Processes and Landforms,* 25, 921-937, 2000.

Braudrick, C.A., Dietrich, W.E., Lecerich, and G.T., Sklar, L.S., Experimental evidence for the conditions necessary to sustain meandering in coarse-bedded rivers, *Proceedings of the National Academy of Sciences,* 106, 40, 16936-16941, 2009.

Daag, A.S., Geomorphic developments and erosion of the Mount Pinatubo 1991 pyroclastic flows in the Sacobia Watershed, Philippines: A study using remote sensing and geographic information systems (GIS), *M.S. thesis, 106 pp., Inernational Institute for Geoinformation Science and Earth Observatory, Enschede, Netherlands*, 1994.

De Baets, S., Poesen, J., Reubens, B., Wemans, K., Baerdemakeker, J.De., and Muys, B., Root tensile strength and root distribution of typical Mediterranean plant species and their contribution to shear soil strength, *Plant Soil,* 305, 207-226, 2008.

Brookes, C.J., Hooke, J.M., and Mant, J., Modelling vegetation interactions with channel flow in river valleys of the Mediterranean region, *Catena,* 40, 93-118, 2000.

Coulthard, T.J., and Van De Wiel, M.J., A cellular model of river meandering, *Earth Surface Processes and Landforms,* 31, 123-132, 2006.

Easson, G., and Yarbrough, L.D., The effects of riparian vegetation on bank stability, *Environmental and Engineering Geoscience*, 8, 4, 247-260, 2002.

Eaton, B.C., and Giles, T.R., Assessing the effect of vegetation-related bank strength on channel morphology and stability in gravel bedded streams using numerical models, *Earth Surface Processes and Landforms,* 34, 712-724, 2009.

Eschner, T.R., Hadley, R.F., Crowley, K.D., Hydrologic and morphologic changes in channels of the Platte River basin in Colorado, Wyoming, and Nebraska: A historical perspective, *U.S. Geological Survey,* A1-A39. 1983.

Ghisalberti, M., Nepf, H.M., Mixing layers and coherent structures in vegetated aquatic flows, *Journal of Geophysical Research,* 107, C2, 2002.

Gran, K.B., and Paola, C., Riparian vegetation controls on braided stream dynamics, *Water Resources Research*, 37, 12, 3275-3283, 2001.

Gran, K.B., Montgomery, D.R., Spatial and temporal patterns in fluvial recovery following volcanic eruptions: Channel response to basin-wide sediment loading at Mount Pinatubo, Philippines. *Geological Society of America Bulletin*, 117 ½, 195-211, 2005.

Gran, K.B., Montgomery, D.R., and Sutherland, D.G., Channel bed evolution and sediment transport under declining sand inputs, *Water Resources Research*, 42, 1-14, 2006.

Gran, K.B., Montgomery, D.R., Halbur, J.C., Long-term elevated post-eruption sedimentation at Mount Pinatubo, Philippines, *Geology*, 39, 367-370. 2011.

Gran,K., Strong seasonality in sand loading and resulting feedbacks on sediment transport, bed structure, and channel planform at Mount Pinatubo, Philippines, Submitted to Earth Surface Processes and Landforms. 30.

Greenway, D.R., Vegetation and slope stability. In: Anderson, M.G., Richards, K.S. (Eds.), Slope Stability, *Geotechnical Engineering and Geomorphology*, Wiley, Chichester, UK, 187–230, 1987.

Hayes, S.K., Montgomery, D.F., and C.G., Newhall, Fluvial sediment transport and deposition following the 1991 eruption of Mount Pinatubo, *Geomorphology*, 45, 211-224, 2003.

Huthoff, F., Augustijn, D.C.M., and Hulscher, J.M.H., Analytical solution of the depth-averaged flow velocity in case of submerged rigid cylindrical vegetation, *Water Resources Research*, 43, 2007.

Liu, D., Diplas, P., Fairbanks, J.D., and Hodges, C.C., An experimental study of flow through rigid vegetation, *Journal of Geophysical Research-Earth Surface*, 113, 2008.

Liu, D., Diplas, P., Hodges, C.C., and Fairbanks, J.D., Hydrodynamics of flow through double layer rigid vegetation, *Journal of Geomorphology*, 116, 286-296, 2010.

James, C.S., Goldbeck, U.K., Patini, A., and Jordanova, A.A., Influence of foliage on flow resistance of emergent vegetation, *Journal of Hydraulic Research*, 46, 4, 536-542, 2008.

Knighton, David. *Fluvial Forms and Processes: A New Perspective*, Hodder Education Press, London, NWI, 1998.

Major, J.J., R.J. Janda, and A.S. Daag, Watershed disturbance and lahars on the east side of Mount Pinatubo during the mid-June 1991 eruptions, in *Fire and Mud: Eruptions and Lahars of Mount Pinatubo, Philippines*, edited by C.G. Newhall and R.S. Punongbayan, 895-919, Philippine Institute of Volcanology and Seismology, Quezon City, Philippines, 1996.

Mattia, C., Bishetti, G., and Gentile, F., Biotechnical characteristics of root systems of typical Mediterranean species, *Plant and Soil*, 278,1, 23-32. 2005.

McBride, M., Hession, C.W., Rizzo, and Donna, M., Riparian reforestation and channel change: A case study of two small tributaries to Sleepers River, northeastern Vermont, USA, *Geomorphology*, 102, 445-459, 2008.

Micheli, E.R., and Kirchner, J.W., Effects of wet meadow riparian vegetation on streambank erosion. 2. Measurements of vegetated bank strength and Consequences for Failure Mechanics, *Earth Surface Processes and Landforms,* 27, 687-697, 2002.

Murray, A.B., and Paola, C., A cellular model of braided rivers, *Nature*, 371, 06492, 54-57, 1994.

Murray, A.B., and Paola, C., Modelling the effect of vegetation on channel pattern in bedload rivers, *Earth Surface Processes and Landforms*, 28, 131-143, 2003.

Murray, A.B., and Paola, C., Properties of a cellular braided-stream model, *Earth Surface Processes and Landforms*, 22, 1001-1025, 1997.

Nicholas, A.P., Cellular modelling in fluvial geomorphology, *Earth Surface Processes and Landforms*, 30, 645-649, 2005.

Paola, C., Parker, G., Mohrig, D.C., Whipple, K.X., The influence of transport fluctuations on spatially averaged topography on a sandy, braided fluvial fan, *Numerical Experiments in Stratigraphy; Recent Advances in Stratigraphic and Sedimentologic Computer Simulations*, edited by J.W. Harbaugh, W.L. Watney, E.C. Rankey, R. Slingerland, R.H., Goldstein, and E.K. Franseen, 211-218, SEPM, Lawrence, 1999.

Papanicolaou, A.N., Diplas, P., Dancey, C.L., and Balakrishnan, M., Surface roughness effects in near-bed turbulence: implications to sediment entrainment, *Journal of Engineering Mechanics*, 127, 3, 211-218, 2001.

Pollen, N., Temporal and spatial variability in root reinforcement of streambanks: Accounting for soil shear strength and moisture, *Catena*, 69, 197-205, 2007.

Pollen-Bankhead, N., and Simon, A., Enhanced application of root-reinforcement algorithms for bank-stability modeling, *Earth Surface Processes and Landforms,* 34, 471-480, 2009.

Pollen, N., and Simon, A., Estimating the mechanical effects of riparian vegetation on stream bank stability using a fiber bundle model, *Water Resources Research,* 41, 1-11, 2005.

Ritter, D.F., Kochel, R.C., Miller, J.R., *Process Geomorphology* 4th edition. Waveland Press, Inc. Long Grove, Illinois, USA. 2002.

Schumm, S.A., Mosley, M.P., Weaver, W.E., *Experimental Fluvial Geomorphology*, Wiley-Interscience, New York, 413 pages, 1987.

Scott,W.E., Hoblitt, R.P., Torres, R.C., Self,S., Martinez, M.M.L., and Nilos, T., Pyroclastic flows of the June 15, 1991, climactic eruption of Mount Pinatubo, in *Fire and Mud: Eruptions and Lahars of Mount Pinatubo, Philippines*, edited by C.G. Newhall and R.S. Punongbayan, 545-570, Philippine Institute of Volcanology and Seismology, Quezon City, Philippines. 1996.

Simon, A., Curini, A., Darby, S.E., Langendoen, E.J., Bank and near bank processes in an incised channel, *Geomorphology*, 35, 183-217, 2000.

Simon, A., and Collison J.C., A., Quantifying the mechanical and hydrologic

effects of riparian vegetation on streambank Stability, *Earth Surface Processes and Landforms*, 27, 527-546, 2002.

Simon, A., Pollen-Bankhead, N., Mahacek, V., and Langendoen, E., Quantifying reductions of mass-failure frequency and sediment loadings from streambanks using toe protection and other means: Lake Tahoe, United States, *Journal of the American Water Resources Association*, 45, 1, 170-186, 2008.

Stoesser, T., Salvador, G.L, Rodi, W., and Diplas, P., Large eddy simulation of turbulent flow through submerged vegetation, *Transport in Porous Media*, 78, 347-365, 2009.

Stone, B.M., Tao Shen, H.T., Hydraulic resistance of flow in channels with cylindrical roughness, *Journal of Hydraulic Engineering*, 128, 5, 500-506, 2002

Takebayashi, H., Okabe, T., Numerical modeling of braided streams in unsteady flow, *Water Management*, 162, WM3, 189-198, 2008.

Tal, M., Gran, K., Murray A.B., Paola, C., and Hicks D.M, Riparian vegetation as a primary control on channel characteristics in Multi-thread Rivers, *Water Science and Application*, 8, 43-57, 2004.

Tal, M., and Paola, C., Dynamic single-thread channels maintained by the interaction of flow and vegetation, *Geological Society of America*, 35, 4, 347-350, 2007.

Thomas, R., Nicholas, A.P., and Quine, T.A., Cellular modeling as a tool for interpreting historic braided river evolution, *Geomorphology*, 90, 302-317, 2007.

Thompson, A.M., Wilson, B.N., and Hansen, B.J., Shear stress partitioning for idealized vegetated surfaces, *American Society of Agricultural Engineers Transactions*, 47, 3, 701-709, 2004.

Thorne, C.R., Effects of vegetation on riverbank erosion and stability, *Vegetation and Erosion*, edited by J.B. Thornes, John and Wiley and Sons, Ltd., 125-144, 1990.

Thorne, C.R., Geomorphic analysis of large alluvial rivers, *Geomorphology*, 44, 3-4, 203-219, 2002.

Tosi, M., Root tensile strength relationships and their slope stability implications of three shrub species in Northern Apennines (Italy), *Geomorphology*, 87, 268-286, 2007.

Tuñgol, N.M., Lahar initiation and sediment yield in the Pasig-Potrero River basin, Mount Pinatubo, Philippines, *Ph.D. thesis, 172, University of Canterbury, Christchurch, New Zealand*, 2002.

Van De Wiel, M.J., Darby, S.E., A new model to analyse the impact of woody riparian vegetation on the geotechnical stability of riverbanks, *Earth Surface Processes and Landforms*, 32, 2185-2198, 2007.

Wilson, C.A.M.E., Stoesser, T., Bates, P.D., and Pinzen, A.B., Open channel flow through different forms of submerged flexible vegetation, *Journal of Hydraulic Engineering*, 129, 11, 847-853, 2003.

Wilson, C.A.M.E., Hoyt, J., and Schnauder, I., Impact of foliage on the drag force of vegetation in aquatic flows, *Journal of Hydraulic Engineering*, 134, 7, 885-891, 2008.

Wu, T.H., McKinnell III, W.P., and Swanston, D.N., Strength of tree roots and landslides on Prince of Wales Island, Alaska, *Canadian Geotechnical Journal*, 16, 19-33, 1979.

Wynn, T.M., Mostaghimi, S., Burger, J., Harpold, A.A., Henderson, M. B., and Henry, L., Ecosystem restoration, variation in root density along stream banks, *Journal of Environmental Quality*, 33, 2030-2039, 2004.

Wynn, T., and M., Saied, The effects of vegetation and soil type on streambank erosion, Southwestern Virginia, USA, *Journal of the American Water Resources Association*, 69-82, 2006.

9. APPENDICIES

9.1. APPENDIX A: NOTATION USED

a = empirically derived coefficient that describes the relationship between root diameter and tensile strength in the RipRoot model

$\frac{A_R}{A}$ = the root area ratio

A_R = area of soil occupied by roots

A = total soil area

$-b$ = empirically derived coefficient that describes the relationship between root diameter and tensile strength in the RipRoot model

B = channel width

B_c = minimum channel flow width in the stem layer

C_D= drag coefficient for a single stem

C_s = constant defined crudely as three times the average slope allowing sediment transport on locally flat or uphill areas, as defined by Murray and Paola (2003)

D_{50} = median grain size obtained from Wolman Pebble Count

d = root diameter

F_v = velocity coefficient defined by Stone and Tao Shen (2002)

g = acceleration due to gravity

h = flow depth

K = vegetation variable used in my cellular model vegetation rule

l^* = wetted stem length/flow depth ratio, assumed to be 1 for equations used

l = wetted stem length

m = exponent based on empirical data relating sediment transport to steam power using reach-averaged slopes, as defined by Murray and Paola (2003)

N = number of stems per unit bed area

Q = initial discharge given to cellular lattice

Q_w = amount of water going into each cell

Q_o= amount of water already present in a cell

Q_s= amount of sediment routed to a cell

Q_{si}= amount of sediment already present in a cell

Q_{sl} = lateral sediment transport in a cell

S = channel slope

S_i = slope of the cells

ΔS = the increased shear strength due to roots

T_r = the average tensile strength of roots per unit area of soil

T_h = sediment-transport threshold, as defined by Murray and Paola (2003)

V = apparent channel velocity

V_c = average channel velocity in the stem layer at constricted section

V_l = average velocity in the stem layer

W = constant used in bedload sediment transport in Murray and Paola (2003)

ρ = density of water

τ_w = the streamwise component of the shear stress

τ_v = the resistance due to the drag around the cylinders within the stem layer

τ_b = the bed shear stress

γ = fraction of the bed that is occupied by vegetation

β = constant of proportionality used in my cellular model sediment transport rule

∂ = constant used in lateral sediment transport in Murray and Paola (2003)

α = constant of proportionality used in my cellular model vegetation rule

9.2. APPENDIX B: MATLAB CODE

```
M=200; %# of rows
N=42; %# of columns
dx=1;
dy=1;
dt=.1;
D=[(dx+dy)^.5 dy (dx+dy)^.5];
T=1000; %Total time of model run
r=1;
g=1;
a=1.5;
%%%Initializes landscape%%%%
z=zeros(M,N);% makes a flat plane
for i=1:M % starting at beginning, counts rows
   for j=1:N % assigns which column
   z(i,j)=i*0.001; % calculate elevation value at each point
   end
end
z=z+rand(M,N)*.00001;% adds random perturbations to elevations
z(:,1)=10;% makes the first column elevation equal to 10
z(:,N)=10; %makes the last column elevation equal to 10
z(:,:)=flipud(z);
z(end,:)=0.00000001;

%%% Initalizes Flow %%%
V=(zeros(M,N,1));
Veff=V-50;
 Veff(Veff<0)=0;



for k=1:T/dt
   clear Q_s
   Q=zeros(M,N,1);% makes a flat plane with all zeros
   Q_s=zeros(M,N);
   Q(1,18:22)=1; %sets flow input
   Q_s(1,18:22)=.1; %sets sediment flux input
   for i=1:M-1; % starting at beginning, counts rows
   Q(:,1)=0;
   Q(:,N)=0;
   q_yes=find(Q(i,:)>0); % finds the cells where there is Q (flow)
   A=size(q_yes); % makes a new variable A which calls out the size of q_yes
      for j=1:A(2); % goes through the q_yes 1 by 1
      B=(q_yes(j)-1:q_yes(j)+1);% names the 3 adjacent cells that you are looking at while routing flow
      S=(z(i,q_yes(j))-z(i+1,B))./D;% calculates slopes in the 3 adj cells
      S(S<0)=.00000001;
      S_min=min(S); %Calculates slope for possible flow paths
      S_yes=S(S>S_min); %defines S_yes as finding the slopes that are more than the minimum slope
```

```
values
48          q_out=B(S>S_min); %names q_out as a new variable pertaining to which cells it outputs to
49          oops=size(S_yes);
50          if oops(2)>0
51
            Q(i+1,q_out(end))=Q(i+1,q_out(end))+Q(i,q_yes(j))*S_yes(end)/(S_yes(1)+S_yes(end)); %using
52      continuity eqn and sqrt of slope ratio, this calculates flow into the 2 destination cells
53          Q(i+1,q_out(1))=Q(i+1,q_out(1))+Q(i,q_yes(j))*S_yes(1)/(S_yes(1)+S_yes(end)); % same as above
54            if Q(i,j) < .1
55            Q(i,j)=0;
56            end
57
58          q_1=a*S_yes(1)*Q(i,q_yes(j))*S_yes(1)/(S_yes(1)+S_yes(end))-Veff(i,q_yes(j))*0.0001;
59          q_2=a*S_yes(end)*Q(i,q_yes(j))*S_yes(end)/(S_yes(1)+S_yes(end))-Veff(i,q_yes(j))*0.0001;
60            if q_1 < 0
61              q_1=0;
62            end
63            if q_2 < 0
64              q_2=0;
65            end
66          Q_s(i,q_yes(j))=Q_s(i,q_yes(j))-q_1-q_2;
67          Q_s(i+1,q_out(end))=Q_s(i+1,q_out(end))+q_2;
68          Q_s(i+1,q_out(1))=Q_s(i+1,q_out(1))+q_1;
69
70          end
71          end
72
73      end
74       V_o=Q==0;
75       V=(V+V_o).*V_o;
76       Veff=V-50;
77       Veff(Veff<0)=0;
78
79       z(:,:)=z(:,:)+Q_s(:,:)*dt;
80       z(end,:)=0.00000001;
81      end
```

9.3. APPENDIX C: VEGETATION PLOT DATA

Sparse Vegetation Plots

Plots		Bank	Species % Cover				Species Characteristics		
Plot #	Location	Bank Height (m)	Grasses	Vines	Woody Trees	Other	Height (m)	Stem Diameter (mm)	# stems
1	PP	1.2	25-50	25-50	0	0	0.1 - 1.0	10	46
2	PP	0.5	0-25	0	0-25	0	1.5-2.0	20	31
3	PP	0.35	0-25	50-75	0	0	1.4	10	16
4	PP	0.3	0-25	25-50	75-100	0-25	1.0-1.5	7	21
5	PP	0	0-25	0	0	0	1.3	10	13
6	PP	0	25-50	0	50-75	0	1.5-3.0	12	17
7	PP	0	0-25	0	0	0	0.5-1.0	5	9
8	PP	0.35	0-25	0	0	0	1.0-2.0	10	20
9	PP	0.35	0	25-50	0	0-25	0.15-0.8	4	14
10	PP	1.3	0-25	50-75	0	0-25	0.7-1.2	7	19
13	PP	1.4	25-50	50-75	0	25-50	1.0-1.9	10	43
14	PP	0	0	0	0	0-25	0.08-0.5	2	5
25	PP	0	75-100	75-100	0	0	1.2-2.6	5	57
26	PP	0	0-25	0	0	0	0.8-1.3	3.5	32
27	PP	0	0-25	0	75-100	0	0.8	17	1
28	PP	0	0-25	0	0	0	6	8	1
29	PP	0	0-25	0	75-100	0	1.5	45	1
1	Sacobia	0.28	0	0	0	0-25	0.1-0.3	no data	no data
5	Sacobia	0	25-50	0	0	0	0.5-1.4	7	31
7	Sacobia	0	0-25	0	0	0	0.3-0.65	5	18
8	Sacobia	0	25-50	0-25	0	0	1.2-2.2	8	12
13	Sacobia	0.31	25-50	0	0	0	0.9-2	10	38
23	Sacobia	0	0-25	0	0	0	0.85-1.3	6	5
34	Sacobia	0	25-50	25-50	0	0	0.5-1.2	4	44
25	Sacobia	0	0-25	0-25	0	0	0.4-1.2	3	16
29	Sacobia	0.45	0-25	0	0	0	0.15-1	7	21
30	Sacobia	0	0-25	0	0	0	1.1-1.2	6	28
31	Sacobia	0.13	25-50	0	0	0	0.6-0.9	5	42
32	Sacobia	0.2	25-50	0	0	0	0.6-1.4	4	54
33	Sacobia	0	25-50	0	0	0	0.4-1.3	5	36

Clumpy Vegetation Plots

Plots		Bank	Species % Cover				Species Characteristics		
Plot #	**Location**	**Bank Height (m)**	**Grasses**	**Vines**	**Woody Trees**	**Other**	**Height (m)**	**Stem Diameter (mm)**	**# stems**
1	PP	0.28	0	0	0	0-25	0.1-0.2	no data	no data
5	PP	0	25-50	0	0	0	0.5-1.4	7	31
7	PP	0	0-25	0	0	0	0.3-0.65	5	18
8	PP	0	25-50	0-25	0	0-25	1.2-2.2	8	35
23	PP	0.31	25-50	0	0	0	0.9-2.0	10	38
24	PP	0	0-25	0	0	0	0.85-1.23	6	5
25	PP	0	0-25	0-25	0	0	0.4-1.2	3	16
29	PP	0.45	0-25	0	0	0	0.15-1	7	21
30	PP	0	0-25	0	0	0	1.1-1.2	6	28
31	PP	0.13	25-50	0	0	0	0.6-0.9	5	42
32	PP	0.2	25-50	0	0	0	0.6-1.4	4	54
33	PP	0	25-50	0	0	0	0.4-1.3	5	36
3	Sacobia	0.61	75-100	0	0	0	no data	5	no data
14	Sacobia	0.17	0	0	0	0	0	0	0
15	Sacobia	0.17	75-100	0	0	0	1.8-4.0	0	0
17	Sacobia	0.35	50-75	0	0	0	0.5-1.2	5	129
26	Sacobia	0	75-100	0	0	0	1.7-3.3	12	57
26B	Sacobia	0	0	0	0	0	0	0	0
27	Sacobia	0	50-75	0	0	0	1.1-2.4	8	48
27B	Sacobia	0	0	0	0	0	0	0	0
28	Sacobia	0	75-100	0	0	0	1.7-3.5	7	52
28B	Sacobia	0	0	0	0	0	0	0	0

Dense Vegetation Plots

Plots		Bank	Species % Cover				Species Characteristics		
Plot #	**Location**	**Bank Height (m)**	**Grasses**	**Vines**	**Woody Trees**	**Other**	**Height (m)**	**Stem Diameter (mm)**	**# stems**
15	PP	0	25-50	75-100	0-25	25-50	0.9-1.8	2.5	85
16	PP	0	50-75	25-50	0	0	0.7-1.5	5	68
17	PP	0	75-100	75-100	0	0	0.8-1.1	4	78
18	PP	0	75-100	25-50	25-50	0	1.8-2.9	7	62
19	PP	0	75-100	50-75	0-25	0	1.3-2.7	10	85
20	PP	0.23	50-75	50-75	75-100	25-50	1.20-2.2	6	55
21	PP	0	75-100	75-100	50-75		1.2-2.4	8	57
22	PP	0.25	50-75	75-100	0	0	1.3-2.7	4.5	45
23	PP	0	75-100	0-25	0-25	0	0.7-2	8	63
24	PP	0	50-75	50-75	0-26	0	1-2.5	9	45
2	Sacobia	0.44	50-75	0-25	0	0	0.8-2.0	19	59
4	Sacobia	0	75-100	50-75	25-50	0	1.4-4.5	13	25
6	Sacobia	0	75-100	75-100	0	0	2.0-4.0	10	55
9	Sacobia	0.4	75-100	0	0	0	1.0-3.0	10	200
10	Sacobia	0.4	75-100	0	0	0-25	0.28-0.3	3	175
11	Sacobia	0.53	25-50	0	0	0	1.5-2.0	5	7
12	Sacobia	0.63	75-100	0	0	50-75	1.2-4.0	8	56
16	Sacobia	0.4	75-100	0-25	0	0	1.1-1.5	6	71
18	Sacobia	0.15	75-100	75-100	0	0	2-2.5	12	82
19	Sacobia	0	50-75	75-100	0	75-100	2.1-3	14	88
20	Sacobia	0	0-25	75-100	0	0	1.3-2.2	8	18
21	Sacobia	0.1	75-100	75-100	0	0	2.05-3.3	15	134

Vegetation plot data were collected on the Pasig-Potrero (PP) and Sacobia braidplains.

9.4. APPENDIX D: ROOT DENSITY DATA

Root Density Data

Sample Name	Species	single or clump	max height (cm)	max diameter (mm)	# stems	Filter Wt (g)	Filter and Roots Wt (g)	Roots Wt (g)	Roots (g/cm3)
T1	Talajib	single	32	3	1	0.98	1.11	0.13	4.64E-05
T2	Talajib	single	61	4	1	1	1.04	0.04	1.43E-05
T3	Talajib	single	101	6	1	0.98	1.06	0.08	2.86E-05
T4	Talajib	single	142	6	1	0.99	1.38	0.39	1.39E-04
T5	Talajib	single	162	6	1	0.97	1.25	0.28	8.27E-04
T6	Talajib	single	206	7	1	0.93	1.34	0.41	4.36E-04
T7	Talajib	clump	67	3	9	0.97	1.27	0.3	2.09E-04
T8	Talajib	clump	88	4	22	0.95	1.44	0.49	1.75E-04
T9	Talajib	clump	119	9	8	1.01	1.08	0.07	2.50E-05
T10	Talajib	clump	161	8	11	0.98	1.32	0.34	1.21E-04
T11	Talajib	clump	202	8	24	0.96	1.82	0.86	3.07E-04
T12	Talajib	clump	250	10	4	0.97	1.25	0.28	1.00E-04
T13	Talajib	clump	303	17	31	0.96	2.91	1.95	6.96E-04
P1	Parasponia	single	65	15	1	0.95	2.61	1.66	5.93E-04
P2	Parasponia	single	120	21	1	0.97	2.26	1.29	1.70E-03
P3	Parasponia	single	196	38	1	0.97	2.37	1.4	1.85E-03
P4	Parasponia	single	64	13	1	0.96	1.52	0.56	2.00E-04
P5	Parasponia	single	173	30	1	0.96	5.73	4.77	1.70E-03
P6	Parasponia	single	40	9	1	0.99	2.13	1.14	2.19E-03

9.5. APPENDIX E: ROOT STRENGTH DATA

Root Strength Data

Sample #	Root Diameter (mm)	Area (m^2)	Max Load (Kgs)	Tensile Strength (MPa)
1	1.50	1.77E-06	1.75	9.88
2	5.10	2.04E-05	2.25	1.10
3	1.60	2.01E-06	2.49	12.41
4	1.30	1.33E-06	1.15	8.65
5	1.40	1.54E-06	1.26	8.16
6	2.80	6.16E-06	1.60	2.59
7	2.00	3.14E-06	0.90	2.86
8	1.50	1.77E-06	0.93	5.26
9	0.60	2.83E-07	0.47	16.52
10	2.60	5.31E-06	2.96	5.57
11	1.80	2.54E-06	1.05	4.12
12	0.70	3.85E-07	0.94	24.40
13	0.70	3.85E-07	0.94	24.40
14	0.70	3.85E-07	0.41	10.61
15	0.50	1.96E-07	0.54	27.72
16	0.90	6.36E-07	0.95	14.97
17	0.50	1.96E-07	0.25	12.94
18	0.70	3.85E-07	1.01	26.17
19	0.30	7.07E-08	0.53	74.44
20	1.50	1.77E-06	0.64	3.64
21	0.80	5.03E-07	0.58	11.55
22	0.90	6.36E-07	1.90	29.80
23	0.90	6.36E-07	0.94	14.83
24	1.00	7.85E-07	0.43	5.49
25	0.60	2.83E-07	0.15	5.29
26	1.60	2.01E-06	0.12	0.59
27	0.70	3.85E-07	0.43	11.20
28	0.50	1.96E-07	0.26	13.17
29	0.30	7.07E-08	0.20	28.88
30	0.20	3.14E-08	0.17	53.42
31	0.40	1.26E-07	0.15	12.27
32	0.90	6.36E-07	0.47	7.42
33	0.40	1.26E-07	0.37	29.60
34	1.30	1.33E-06	0.49	3.66
35	0.40	1.26E-07	0.03	2.17
36	1.30	1.33E-06	0.97	7.28
37	0.60	2.83E-07	0.32	11.23
38	0.40	1.26E-07	0.18	14.08
39	1.00	7.85E-07	0.09	1.16
40	0.40	1.26E-07	0.33	26.35

Root Strength Data condt.

Sample #	Root Diameter (mm)	Area (m^2)	Max Load (Kgs)	Tensile Strength (MPa)
41	0.50	1.96E-07	0.60	30.72
42	0.70	3.85E-07	0.36	9.43
43	1.00	7.85E-07	0.25	3.18
44	0.70	3.85E-07	1.32	34.18
45	0.70	3.85E-07	0.05	1.18
46	0.60	2.83E-07	0.21	7.38
47	1.10	9.50E-07	0.32	3.39
48	0.80	5.03E-07	1.72	34.20
49	0.40	1.26E-07	0.91	72.19
50	0.50	1.96E-07	0.18	9.01
51	1.70	2.27E-06	1.44	6.35
52	0.30	7.07E-08	0.34	48.13
53	0.70	3.85E-07	0.53	13.79
54	0.40	1.26E-07	1.37	108.65
55	0.50	1.96E-07	1.15	58.45
56	1.50	1.77E-06	1.88	10.63
57	0.60	2.83E-07	0.85	30.16
58	0.60	2.83E-07	0.55	19.41
59	0.10	7.85E-09	0.10	127.32
60	0.60	2.83E-07	0.73	25.67
61	0.70	3.85E-07	0.27	6.95
62	0.60	2.83E-07	0.25	8.82
63	1.30	1.33E-06	1.21	9.09
64	0.30	7.07E-08	0.25	35.94
65	0.60	2.83E-07	1.69	59.68
66	1.00	7.85E-07	1.23	15.71
67	0.60	2.83E-07	1.49	52.78
68	0.20	3.14E-08	0.35	111.17
69	0.70	3.85E-07	1.67	43.37
70	1.30	1.33E-06	1.02	7.65
71	0.50	1.96E-07	0.78	39.50
72	0.40	1.26E-07	0.64	51.26
73	0.50	1.96E-07	0.65	33.03
74	0.30	7.07E-08	0.52	73.15
75	0.30	7.07E-08	0.69	98.18
76	0.30	7.07E-08	0.78	110.37
77	0.30	7.07E-08	0.39	55.83
78	1.10	9.50E-07	1.71	17.99
79	1.40	1.54E-06	2.01	13.08
80	1.20	1.13E-06	0.30	2.65

Root Strength Data condt.

Sample #	Root Diameter (mm)	Area (m^2)	Max Load (Kgs)	Tensile Strength (MPa)
81	1.10	9.50E-07	0.51	5.39
82	1.80	2.54E-06	0.97	3.81
83	0.50	1.96E-07	1.16	58.91
84	0.60	2.83E-07	1.53	54.06
85	0.50	1.96E-07	0.83	42.51
86	0.80	5.03E-07	1.56	30.95
87	0.20	3.14E-08	0.10	31.83
88	1.10	9.50E-07	1.09	11.46
89	1.40	1.54E-06	0.93	6.04
90	1.30	1.33E-06	1.32	9.91
91	1.00	7.85E-07	0.46	5.89
92	1.10	9.50E-07	0.26	2.77
93	1.20	1.13E-06	1.13	10.03
94	1.00	7.85E-07	1.56	19.92
95	0.50	1.96E-07	0.37	18.71
96	1.00	7.85E-07	0.95	12.07
97	0.70	3.85E-07	1.42	36.89
98	0.80	5.03E-07	0.32	6.41
99	1.20	1.13E-06	0.92	8.10
100	1.90	2.84E-06	2.10	7.41
101	2.30	4.15E-06	2.10	5.05
102	1.60	2.01E-06	0.95	4.72
103	0.60	2.83E-07	0.50	17.81
104	1.30	1.33E-06	0.95	7.14
105	1.20	1.13E-06	1.13	10.03
106	0.60	2.83E-07	0.47	16.68
107	1.10	9.50E-07	0.25	2.63
108	0.80	5.03E-07	0.33	6.59
109	1.20	1.13E-06	0.85	7.50
110	1.50	1.77E-06	1.66	9.39
111	0.90	6.36E-07	1.56	24.46
112	1.30	1.33E-06	0.70	5.30
113	0.60	2.83E-07	0.55	19.41
114	1.10	9.50E-07	1.49	15.70
115	0.90	6.36E-07	0.83	12.98
116	1.30	1.33E-06	2.00	15.07
117	0.30	7.07E-08	0.31	44.28
118	0.70	3.85E-07	1.53	39.72
119	0.50	1.96E-07	0.40	20.56
120	0.50	1.96E-07	0.48	24.49

Root Strength Data condt.

Sample #	Root Diameter (mm)	Area (m^2)	Max Load (Kgs)	Tensile Strength (MPa)
121	0.80	5.03E-07	0.30	6.05
122	0.50	1.96E-07	0.84	42.74
123	0.30	7.07E-08	0.38	53.90
124	0.20	3.14E-08	0.34	109.73
125	0.30	7.07E-08	0.34	48.13
126	0.40	1.26E-07	0.83	65.69
127	0.50	1.96E-07	0.82	41.81
128	0.10	7.85E-09	0.18	231.01
129	0.20	3.14E-08	0.29	93.85
130	0.10	7.85E-09	0.10	127.06
131	0.50	1.96E-07	0.07	3.70
132	0.70	3.85E-07	0.35	9.19
133	1.30	1.33E-06	0.42	3.18
134	0.90	6.36E-07	0.77	12.05
135	0.50	1.96E-07	0.22	11.09
136	0.70	3.85E-07	0.90	23.45
137	0.70	3.85E-07	0.87	22.63
138	0.50	1.96E-07	0.44	22.41
139	0.80	5.03E-07	1.34	26.62
140	0.80	5.03E-07	0.87	17.33
141	0.60	2.83E-07	0.48	17.01
142	0.80	5.03E-07	1.07	21.21
143	0.30	7.07E-08	1.76	249.62
144	0.70	3.85E-07	1.76	45.73
145	1.00	7.85E-07	1.51	19.17
146	0.20	3.14E-08	0.23	73.64
147	1.00	7.85E-07	1.31	16.63
148	0.70	3.85E-07	2.20	57.16
149	1.30	1.33E-06	2.04	15.34
150	0.30	7.07E-08	0.15	21.82
151	0.20	3.14E-08	0.17	53.42
152	0.90	6.36E-07	1.81	28.52
153	0.60	2.83E-07	0.82	28.88
154	0.30	7.07E-08	0.02	3.21
155	0.20	3.14E-08	0.34	108.29
156	0.90	6.36E-07	1.35	21.25
157	0.50	1.96E-07	0.60	30.72
158	0.60	2.83E-07	1.24	43.80
159	1.10	9.50E-07	2.12	22.34

Root Strength Data condt.

Sample #	Root Diameter (mm)	Area (m^2)	Max Load (Kgs)	Tensile Strength (MPa)
160	1.90	2.84E-06	1.81	6.38
161	0.80	5.03E-07	0.68	13.63
162	0.70	3.85E-07	0.35	9.08
163	0.60	2.83E-07	1.98	69.95
164	0.50	1.96E-07	0.86	43.89
165	0.60	2.83E-07	1.05	37.06
166	0.50	1.96E-07	0.27	13.63
167	0.90	6.36E-07	0.59	9.34
168	0.70	3.85E-07	0.63	16.27
169	0.60	2.83E-07	0.32	11.23
170	0.30	7.07E-08	0.86	121.28
171	0.70	3.85E-07	0.39	10.02
172	0.40	1.26E-07	0.17	13.36
173	0.10	7.85E-09	0.14	173.26
174	0.70	3.85E-07	0.36	9.31
175	1.00	7.85E-07	0.50	6.41
176	0.20	3.14E-08	0.05	14.44
177	0.70	3.85E-07	0.34	8.84
178	0.60	2.83E-07	0.26	9.14
179	0.60	2.83E-07	0.41	14.44
180	0.70	3.85E-07	0.39	10.25
181	0.40	1.26E-07	0.40	32.13